Advances in Redox Research 15 (2025) 100126

Contents lists available at ScienceDirect

Advances in Redox Research

journal homepage: www.elsevier.com/locate/arres

Full Length Article

Repurposing *Bacopa monnieri* extracts containing Aquaporin-1 blockers to improve systemic oxidative stress: The BacOxy_I study

Hasnae Boughaleb [a], Roxane Verdoy [a], Amandine Pochet [b], Nathalie Fabian [a], Ramona Bella [a], Gopinath Muruganandam [a], Raphaël Frédérick [c], Karim Zouaoui Boudjeltia [d], Axelle Bourez [e], Cédric Delporte [e], Pierre Van Antwerpen [e], Annie Robert [f], Vincent Haufroid [g], Joseph P. Dewulf [b,g], Jean-Luc Balligand [a,h], Virginie Montiel [a,i,*]

[a] *Pole of Pharmacology and Therapeutics (FATH), Institute of Experimental and Clinical Research (IREC), Université Catholique de Louvain (UCLouvain), Brussels, Belgium*
[b] *Louvain Centre for Toxicology and Applied Pharmacology (LTAP), Institute of Experimental and Clinical Research (IREC), Université Catholique de Louvain (UCLouvain), Brussels, Belgium*
[c] *Louvain Drug Research Institute (LDRI), Université Catholique de Louvain (UCLouvain), Brussels, Belgium*
[d] *Laboratoire de Médecine Expérimentale (ULB 222), Université Libre de Bruxelles, Medicine Faculty, CHU Charleroi-Chimay, Belgium*
[e] *RD3-Pharmacognosy, Bioanalysis and Drug Discovery & Analytical Platform of the Faculty of Pharmacy, Université Libre de Bruxelles, Brussels, Belgium*
[f] *Pole of Epidemiology & Biostatistics (EPID), Institute of Experimental and Clinical Research (IREC), Université Catholique de Louvain (UCLouvain), Brussels, Belgium,*
[g] *Department of Clinical Chemistry, Cliniques Universitaires Saint-Luc, UCLouvain, Brussels, Belgium*
[h] *Department of Internal Medicine, Cliniques Universitaires Saint-Luc, Brussels, Belgium*
[i] *Intensive care unit, Cliniques Universitaires Saint-Luc, Brussels, Belgium*

ARTICLE INFO

Keywords:
Oxidative stress
Reactive oxygen species (ROS)
Endothelial dysfunction
Aquaporin 1 (AQP1)
Bacopaside II
Bacopa monnieri

SUMMARY

Objectives: To evaluate the efficacy of Bacopa monnieri (BM) containing Bacopaside II, a specific Aquaporin 1 (AQP1)-blocker, on **systemic** oxidative stress.
Background: AQP1, is a peroxiporin which facilitates hydrogen peroxide transmembrane passage. It is predominantly expressed in endothelial cells and erythrocytes.
Methods: BM extract was administered orally for 6 weeks to 20 healthy volunteers (Group A/B: 400/800 mg/day). Assessments occurred at baseline (V0), after 6 weeks of treatment (V4), and 4 weeks post-treatment (V6). Primary endpoint: ROS levels in erythrocytes post-H_2O_2 exposure (DCFDA fluorescence). Secondary endpoints: Oxidative stress and safety biomarkers, blood pressure monitoring. Bacopaside II metabolites in plasma were identified using liquid chromatography-mass spectrometry (LC-MS).
Results: BM intake reduced ROS levels in RBCs in Group B (T40 min: Mean Fluorescence Intensity of DCF V0=381 ± 43 a.u vs V4= 187 ± 69 a.u, $p<0.01$). Methemoglobin and oxidized Methionine 148 of Apolipoprotein A-1 levels decreased (Methemoglobin group B: V0= 0.900 ± 0.105 a.u vs V4= 0.233 ± 0.047 a.u; $p<0.001$, M148-ox/M148 ratio group B: V0= 0.06 ± 0.01 a.u. vs V4= 0.02 ± 0.00 a.u.; $p<0.05$). A reduction in blood pressure was observed in Group B (Systolic Blood Pressure V0=131 ± 15 mmHg vs SBP V4=116 ± 7 mmHg; $p < 0.05$). Two potential Bacopaside II metabolites with putative binding pockets on AQP1 were identified during the treatment.
Conclusion: A six-week oral intake of BM reduced **systemic** oxidative stress in healthy volunteers in a dose-dependent manner. Pharmacological blocking of AQP1 may help restore redox balance in the vasculature.

* Corresponding author.
E-mail address: virginie.montiel@saintluc.uclouvain.be (V. Montiel).

https://doi.org/10.1016/j.arres.2025.100126
Received 25 January 2025; Received in revised form 17 March 2025; Accepted 17 March 2025
Available online 20 March 2025

Abbreviations

ApoA1	apolipoprotein A1
ApoB-100	apolipoprotein B100
AQP	aquaporin
BH_4	tetrahydrobiopterin
BM	Bacopa monnieri
CVD	cardiovascular diseases
DCF	2′,7′-Dichlorofluorescein
eNOS	endothelial nitric oxide synthase
H_2-DCFDA	chloromethyl dichlorofluorescein diacetate
H_2O_2	hydrogen peroxide
MetHb	methemoglobin
MFI	mean fluorescence inyensity
Mox-HDL	Myeloperoxidase-associated oxidation of Apolipoprotein A-1 on High-Density Lipoprotein.
Mox-LDL	Myeloperoxidase-associated oxidation of Apolipoprotein B-100 on Low-Density Lipoprotein
MPO	myeloperoxidase
NO	nitric oxide
O_2^-	superoxide anion
RBCs	red blood cells
ROS	reactive oxygen species

1. Introduction

The primary risk factors for cardiovascular diseases (CVD)—e.g. hypertension, obesity, smoking and dyslipidemia—lead to the development of atherosclerosis [1]. Atherosclerosis, in turn, underlies severe ischemic cardiovascular diseases leading to substantial mortality [2]. In 2020, CVD accounted for 1.7 million deaths in Europe, representing one-third of all deaths [3].

The vascular endothelium, a monolayer comprising over 10^{14} endothelial cells, is the largest organ in the human body and is highly sensitive to reactive oxygen species (ROS) signaling. In physiological conditions, small amounts of ROS activate pathways involved in angiogenesis, endothelial permeability, and vasorelaxation. However, excessive ROS production impairs endothelial function, in part by disrupting the nitric oxide (NO) pathway [4]. Such endothelial dysfunction is a key contributor to the development of atherosclerosis and cardiovascular pathologies, notably heart failure and stroke [2].

Endothelial dysfunction classically results from an imbalance between NO produced by endothelial nitric oxide synthase (eNOS) and ROS produced by NADPH oxidase-2 (Nox)-2 or uncoupled eNOS [5]. In turn, ROS can interfere with NO-dependent signaling at multiple sites, through, e.g. oxidation of soluble guanylate cyclase altering its responsiveness to NO; formation of peroxynitrite reducing the bioavailability of NO itself; or "uncoupling" of NOS converting it into an O_2^--generating enzyme [6]. Such disruption in the vessel redox signaling initiates a chain of events involving endothelial "activation", sub-endothelial inflammation, vasoconstriction, thrombosis and plaque rupture, culminating in vessel occlusion [7].

Oxidant stress stems from the production of free radicals, including superoxide anion and hydroxyl radical, as well as more stable non-radicals, such as hydrogen peroxide (H_2O_2), that are not adequately countered by antioxidant systems [8]. Due to its relative stability H_2O_2 alternates in a concentration-dependent manner from physiological to pathological signaling, the latter through non-specific oxidation of DNA, proteins, lipids or other macromolecules and pro-apoptotic signaling pathways [9]. Moreover, H_2O_2 is used by peroxidase, namely myeloperoxidase (MPO), to produce hypochlorous acid, a highly reactive pro-oxidant species.

Mammalian aquaporins (AQPs) belong to a family of thirteen isoforms (AQP0-AQP12) of water channels, the first of which, Aquaporin 1 (AQP1) was discovered by P. Agre and his colleagues in 1992 [10]. AQPs facilitate the rapid transmembrane transport of water, playing pleiotropic roles in fluid transport, brain water balance, cell migration, proliferation, and epidermal hydration [11].

AQP1 is the main isoform expressed in cardiovascular (CV) tissues of mammals [12] and is strongly expressed in all resident cell types including cardiac myocytes, vascular smooth muscle cells and endothelial cells [13]. AQP1 is organized as a homotetramer in which each subunit behaves as an independent functional water channel. This water channel also has a central pore at the level of the fourfold symmetry axis in the tetramer involved in cation conduction, whose physiological role remains to be determined [14]. A new function of AQP1 in cardiovascular tissues was suggested when we confirmed AQP1 as a *bona fide* "peroxiporin" in mammalian cells, akin to other isoforms, including AQP3, AQP5, AQP8, AQP9 and AQP11. As the passage of H_2O_2 across the membrane is limited, these "peroxiporins" facilitate the bidirectional transport of H_2O_2 across cellular membranes (in addition to water), thereby playing critical roles in oxidative stress signaling [15]. Indeed, we identified AQP1 as a part of a "signalosome" that mediates cardiac hypertrophy by specifically facilitating the transmembrane passage of extracellular H_2O_2 in the caveolae [16]. The identification of AQP1 as a peroxiporin, particularly with its high expression at the endothelial level, suggests its potential involvement in vascular oxidative stress and the subsequent ROS-dependent endothelial dysfunction. This highlights AQP1 blockade as a promising therapeutic approach for the prevention or treatment of endothelial dysfunction.

Indeed, AQP1 conductance can be modulated by specific inhibitors such as Bacopaside II. Blockade of AQP1 has demonstrated significant potential in the oncology field by reducing tumor growth, migration, and invasion in various cancer cell lines [17,18]. Bacopaside II belongs to the pseudojujubogenin group of the saponin family [19]. These compounds are characterized by a triterpenoid aglycone moiety linked to one or more sugar chains, with the sugar component conferring specificity to each member of the pseudojujubogenin family, distinguishing, e.g., Bacopaside I from Bacopaside II [20]. Our previous study showed that the in vitro blockade of AQP1 using Bacopaside II, attenuates the transmembrane passage of H_2O_2 into mouse cardiac myocytes [16]. However, Bacopaside II is difficult to purify and costly, which limits its application in large quantities for in vivo studies.

Bacopa monnieri (BM) is a common plant that has been used in Ayurvedic medicine for millenaries for the treatment of diverse chronic neurological diseases through poorly characterized mechanisms [20] . This plant is known to contain Bacosides of which Bacopasides I and II are recognized as specific inhibitors of AQP1 [17]. While Bacopaside I inhibits both the monomeric water channels and the central pore, Bacopaside II is specific to the water channel [17], that is responsible for transporting H_2O_2.

Therefore, this study aimed to test the applicability of AQP1 blockade **on oxidative** stress in healthy volunteers by using oral administration of the Bacopa-400® BM extract. Direct assessment of H_2O_2 passage in cardiovascular tissues in vivo is not feasible. Thus, we used red blood cells (RBCs) as *proxy* for endothelial cells due to their high expression of AQP1 and wide exposure to the vascular biological milieu [21].

2. Material and methods

2.1. Design of the clinical study

This open-label, interventional, and monocentric study was conducted at Cliniques Universitaires Saint Luc/UCLouvain (Brussels). The study enrolled two parallel groups of 10 healthy volunteers administered two doses of BM extracts (400 mg and 800 mg/d), known as Bacopa-400®. The treatment duration was 6 weeks, followed by a 4-week observation period after treatment cessation. The study results are presented according to the STROBE cohort reporting guidelines [22].

Bacopa-400® is a standardized extract of BM plant, comprising 45 %

dry weight of mixed Bacosides, including Bacopaside II. This BM extracts is marketed by the Belgian firm Deba Pharma™ according to Good Manufacturing Practice (GMP) criteria.

2.2. Ethics

The study protocol was approved by the ethical committee (Comité d'Ethique Hospitalo-Facultaire, Cliniques Saint-Luc) and was registered in ClinicalTrials.gov (NCT06355167).

2.3. Patients

In this study, we included adult healthy volunteers (≥18 years) and excluded volunteers taking any chronic medication for a chronic disease or any dietary supplements, pregnant or breastfeeding women and patients with gastric problems (e.g. ulcer, gastro-esophageal reflux, lactose intolerance). Volunteers were excluded if they were suffering from an acute infection at any time during the study and they were not allowed to start ant other food supplement during the study. Particular care was taken in detecting infection with COVID-19, which is known to impair endothelial function [23]. Every volunteer signed an informed consent form before the beginning of the study.

2.4. Sample size

Using PASS 14 (Power Analysis and Sample Size Software (2015). NCSS, LLC. Kaysville, Utah, USA, ncss.com/software/pass), we found that to achieve an effect size of 1.5 with a power of 90 % and α level of 0.05 using a non-paired *t*-test, we needed 7 volunteers/group. In order to anticipate potential dropouts, we opted to recruit an additional 3 volunteers per group, resulting in a total of 10 volunteers per group or 20 volunteers for the entire study. Furthermore, to ensure balanced groups, we included an equal number of male and female participants in each group, with 5 males and 5 females per group. Finally, as this was a pilot study, no randomization criteria, such as age stratification, were applied in the sample size calculation, allowing the inclusion of participants across all age groups.

2.5. Schedule of the study

The recruitment occurred at Cliniques Universitaires Saint Luc between February 2022 and April 2022, resulting in a total of 20 volunteers, comprising 10 males and 10 females (Table 1). Volunteers were assigned a numerical identifier based on their chronological enrollment, with even-numbered volunteers allocated to group A (400mg/d) and odd-numbered volunteers assigned to group B (800mg/d). The schedule of the study is described in Fig. 1.

The study lasted 10 weeks, including a 6-week treatment period (from April to June 2022) with BM extracts (Bacopa-400®). Outcomes assessments involved blood sampling, urine tests, and blood pressure measurements, which were repeated at baseline (V0, 2 weeks (V2) and 6 weeks (V4) post-treatment initiation. Subsequently, a final assessment was conducted 4 weeks after the completion of treatment (V6). Detailed descriptions of all biological tests conducted during the study are provided in Table 2. During the study duration, volunteers completed online questionnaires at different time points to report any adverse events (from V1 to V6) (cf. Fig. 1).

Table 1
Allocation of groups.

Groups	n	Sex ratio	Dose of Bacopa-400®/day
A	10	1:1	400 mg
B	10	1:1	800 mg

2.6. Blood sampling

Blood samples were collected from fasting healthy volunteers, in the same time for each group (between 8 and 10 am), using EDTA tubes and processed with precision according to the specific requirements of each experiment. The detailed methodologies for sample handling and analysis are provided in Sections 2.7, 2.9, 2.10, and 2.11.

2.7. Assessment of Bacopaside II in Bacopa-400® plant extract and its potential metabolites in the plasma of healthy volunteers: Metabolite extraction and liquid chromatography-mass spectrometry analysis

Liquid-liquid extractions and Liquid chromatography-mass spectrometry (LC-MS) analyses were based on a method previously described [24] Metabolites from plasma samples (100 µl) were extracted after the addition of 300 µl of acetonitrile MS-grade (Biosolve) containing digitoxin at 10 nmol/l (Sigma-Aldrich D5878) used as internal standard. The samples were thoroughly mixed, sonicated and incubated at -20 °C for 30 min, then centrifuged at 10,000g for 10 minutes at 4 °C. The upper-phase (200 µl) was collected and 300 µl of acetonitrile were added to the initial sample for a second similar extraction, followed by 300 µl collection of the upper-phase. A volume of 125 µl of the combined liquid extract collection was dried down under a gentle stream of nitrogen at 30 °C and kept frozen until analysis. Liquid-liquid extraction from Bacopa-400® (10 mg powder) was also performed. Briefly, the powder was mixed with 200 µl of MS-grade water (Biosolve), followed by two successive extractions using 600 µl of pure acetonitrile. Prior to analysis, the samples were reconstituted in [water: acetonitrile, 1:1, 0.1% formic acid]. The tubes were centrifuged at 10,000g for 5 minutes at 4 °C to remove any particulates before being transferred into polypropylene autosampler vials. Three microliters of each reconstituted sample were injected and subjected to reverse phase liquid chromatography using an UPLC ACQUITY Premier system (Waters) in negative ionization mode. The separation column, operated at 40 °C, was an Acquity Premier HSS T3 column 1.8 µm, 2.1 × 100 mm (Waters). Liquid chromatography was performed using a binary mobile phase system. Mobile phase A consisted of water with 0.1 % acetic acid (Biosolve) and phase B consisted of acetonitrile with 0.1% acetic acid. The reverse phase separations were performed at 0.5 mL/min with an isocratic period of 1 min at 99 % A, followed by three consecutive linear gradients: from 1 % B to 15 % B over 2 min, from 15 % B to 50 % B over 3 min and from 50 % B to 95 % B over 3 min. The final composition of 95 % B was held constant for 4 min followed by a return to 99 % A, kept for 1 min. Mass spectrometry data was acquired in profile (continuum) format over the mass range of *m/z* 50–1200 using a Waters Synapt-XS high resolution Q-TOF mass spectrometer set in MS^E resolution mode: scan time 0.1 sec, the low and high trap collision energy were 4 V and a ramp between 20 and 50 V, respectively. An electrospray ionization (ESI) source was used in negative mode. Capillary and sampling cone voltages were set to 2 kV and 25 V, respectively. Source temperature was set to 150 °C and desolvation temperature to 550 °C. Gas flow rates were set at 1100 L/h for the desolvation gas and 50 L/h for the cone gas. Acquisition of leucine enkephalin infused at 10 µl/min through a lockspray probe allowed a real time mass correction (30 sec scan intervals). Raw LC-MS data (MassLynx software acquisition) were imported and processed in Waters connect (Unifi version 1.9.13.9). Next to the targeted analysis of Bacopaside II ($C_{47}H_{76}O_{18}$, $[M+CH_3COO]^-$ 987.517 *m/z*, retention time 6.4 min) and digitoxin ($C_{41}H_{64}O_{13}$, $[M+CH_3COO]^-$ 823.445 *m/z*, retention time 7.2 min) from blood samples and Bacopa-400® extracts, computational simulation analysis of MS raw data was performed applying the transformation processing tool in Unifi, looking for the presence of putative peaks in chromatograms corresponding to exact mass of metabolized metabolites from Bacopaside II after phase I (n = 0, 1 or 2) and/or phase II (n = 0 or 1) transformation(s): desaturation ($-H_2$), reduction ($+H_2$), oxidation (+O), glucuronidation ($+C_6H_8O_6$), glutathione S-conjugation ($+C_{10}H_{15}N_3O_6S$), acetylation ($+C_2H_2O$) and sulfation

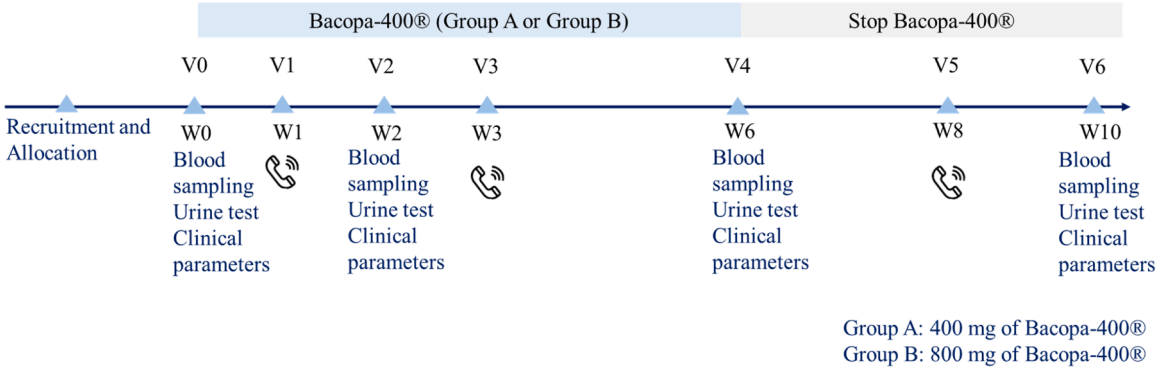

Fig. 1. Schedule of the study. NB: The phone represents the phone calls and online questionnaires to report the adverse events.

Table 2
Description of analyses during the study.

Visits	V0	V1	V2	V3	V4	V5	V6
Week	0	1	2	3	6	8	10
Bacopa-400®	X	X	X	X	X		
Assessment of Bacopaside II potential metabolites in the plasma							
LC-MS	X				X		X
Assessment of antioxidant potential of Metabolites in the plasma							
Amplex-red	X				X		
Oxidative stress assessment							
DCFDA assay	X		X		X		X
Methemoglobin	X				X		X
Plasma peroxides	X		X		X		X
Myeloperoxidase activity products	X				X		X
Oxidized Apolipoproteins	X				X		X
Clinical and biologic safety assessment							
Blood pressure	X		X		X		X
Hepatic function (ASAT, ALAT, GGT)	X		X		X		X
Muscular damage enzymes LDH, CPK	X		X		X		X
Renal function (creatinine, urea)	X		X		X		X
Hemogram	X		X		X		X
Ionogram	X		X		X		X
Lipogram	X		X		X		X
Urinary sediments	X		X		X		X
Proteinuria	X		X		X		X
Adverse Event (AE) assessment							
AE and SUSAR	X	X	X	X	X	X	X

AE: Adverse Events; ALAT: alanine aminotransferase; ASAT: aspartate aminotransferase; CPK: creatine phosphokinase; DCFDA: 2′,7′-dichlorofluorescin diacetate; GGT: gamma-glutamyl transferase; LC-MS: liquid chromatography-mass spectrometry; LDH: lactate dehydrogenase; MPO: myeloperoxidase; SUSAR: Suspected Unexpected Serious Adverse Events.

($+SO_3$). The signal of discovered metabolites was compared in plasma extracts of volunteers based on the ratio between the area under the curve of the metabolites and digitoxin, used as internal standard.

2.8. Molecular docking

To explore the potential binding sites of the Bacopaside II metabolites on AQP1 in silico, molecular docking was performed using Molecular Operating Environment (MOE), 2022.02 Chemical Computing Group ULC, 910–1010 Sherbrooke St. W., Montreal, QC H3A 2R7, Canada, 2024. Prior to docking, a three-dimensional (3D) crystal structure of human AQP1 was retrieved from Protein Data Bank [PDB ID: 1J4N]. Co-crystallized water molecules were removed, and hydrogen atoms were added to the protein with Protonate 3D Wizard of MOE. The protein was energy minimized with a root mean square gradient of 0.1 kcal/mol/A2 with Merck Molecular Force Field (MMFF94), implemented in MOE minimization module, to relax atom coordinates and prevent atomic clashes [25]. Two-dimensional (2D) structures of the metabolites were drawn in ChemDraw 19.1 (PerkinElmer Informatics), transferred to MOE where their 3D coordinates were generated using the Molecular Builder interface of MOE. The generated 3D structures were subjected to energy minimization to the above gradient using the MMFF94 force field. Theoretical binding pockets on AQP1 were found by applying the Site Finder tool of MOE. Rigid receptor approach was used for docking. Conformations were chosen based on binding energy and docking scores.

2.9. ROS detection in human erythrocytes by DCFDA assay

Chloromethyl dichlorofluorescein diacetate (CM-H2DCFDA, Invitrogen C6827) served as a probe to quantify intracellular reactive oxygen species (ROS) such as H_2O_2. Throughout this paper, CM-H_2DCFDA will be referred to as H_2-DCFDA. After passive diffusion into the cells and upon encountering ROS, H_2-DCFDA undergoes conversion to produce a highly fluorescent compound, the DCF (2′,7′-Dichlorofluorescein). This resulting fluorescence intensity was quantified using Fluorescence-Activated Cell Sorting (FACS, BD FACS Canto II) and represented as DCF mean fluorescence intensity (MFI) in the graphs. The excitation and emission wavelength used were respectively 488 and 530 nm.

a) **Modulation of the kinetics of transmembrane passage of H_2O_2 in Red Blood Cells exposed *ex vivo* to purified Bacopaside II**

Following blood collection in EDTA tubes, centrifugation was performed for 10 minutes at 800 g to separate plasma from red blood cells (RBCs). The RBCs (diluted 1:1000 in Hanks' Balanced Salt solution HBSS) were incubated with 10 μM Bacopaside II (Supelco, Sigma-Aldrich 44,698) for 1 hour at room temperature in the dark. Then RBCs were loaded with 1.5 μM of H_2-DCFDA for 30 min at 37 °C in presence of 50 μM of 3-AT (3-Amino-1,2,4-triazole, Sigma-Aldrich A8056) to inhibit the intracellular catalase. The RBCs were centrifuged and suspended again in fresh HBSS for removing excess extracellular H_2-DCFDA. After a basal reading, 15 μM of H_2O_2 (Sigma-Aldrich H1009) or vehicle (HBSS) was added to the RBCs, leading to the formation of the fluorescent compound DCF. The time-dependent increase in DCF MFI was monitored over a 25-minute period, with initial readings taken at 0 and 1 minute, followed by measurements every 6 minutes up to 25 minutes. The level of intracellular ROS was directly proportional to the intensity of DCF fluorescence, providing a direct measure of the relative ROS quantity. Variations in DCF fluorescence were represented as standardized DCF MFI and SEM calculated by subtracting the basal DCF MFI from the DCF MFI of RBCs exposed to H_2O_2. This experiment was repeated on RBCs of 4 volunteers.

b) **Kinetics of transmembrane passage of H_2O_2 in Red Blood Cells *ex vivo* after oral intake of Bacopa monnieri extracts**

The same H_2-DCFDA loading protocol was used for these experiments. Then, the RBCs freshly drawn from subjects who had taken BM extracts orally were exposed to either a concentration of 10 μM of H_2O_2 (Sigma-Aldrich H1009), or vehicle (control RBCs in HBSS). The time-dependent increase in DCF MFI was monitored over a 40-minute period, with readings taken at 0–7–13–19–25–31 and 40 min. Variations in DCF fluorescence were depicted as standardized DCF MFI and SEM, calculated by subtracting the control DCF MFI (unexposed to H_2O_2) from the DCF MFI of RBCs exposed to H_2O_2. This method allowed specific measurements of treatment-induced changes in MFI while minimizing background noise. To reduce inter-variability due to the limited number of patients and high variability in DCFDA response between patients, baseline (pre-treatment) standardized DCF MFI values of groups A and B were pooled. Subsequent comparisons were made between pooled baseline (V0) values and standardized DCF MFI values at V4 and V6 for groups A and B, respectively.

2.10. Assessment of direct antioxidant effect of Bacopa monnieri and its metabolites

The antioxidant effect was assessed using the Amplex Red assay, which uses 10-acetyl-3,7-dihydroxyphenoxazine. In this assay, horseradish peroxidase (HRP) catalyzes the conversion of Amplex Red to the fluorescent compound resorufin in the presence of hydrogen peroxide (H_2O_2). This technique was applied to plasma samples to determine whether potential metabolites of BM extracts in the plasma would directly scavenge H_2O_2 rather than interfering with AQP1 channel permeability.

Blood was collected in EDTA tubes and centrifuged at 800g for 10 minutes to separate plasma, which was then promptly frozen at -80 °C. Before experimentation, plasma samples were diluted (1:5 in HBSS). To minimize interference from endogenous catalase activity, the inhibitor 3-amino-1,2,4-triazole (3-AT, Sigma-Aldrich A8056) was added at a concentration of 5mM and incubated for 10 minutes. Subsequently, 40 μL of each sample was pipetted into the wells of a microplate plus 200 μM H_2O_2 or vehicle (HBSS) solution.

The Amplex Red reaction mixture, freshly prepared with Amplex Red reagent (final concentration: 50 μM), HRP (final concentration: 0.1 U/mL), and HBSS, was then added to the diluted plasma samples to initiate the reaction. These were incubated at 37 °C for 30 minutes. Fluorescence emission, indicative of the reaction of H_2O_2 with Amplex red reaction mixture, was quantified using a SpectraMax i3X (Molecular device) with excitation and emission wavelengths set at 560 nm and 590 nm, respectively. For each volunteer, a sample without H_2O_2 served as a control (vehicle HBSS), and data were normalized as the ratio of samples with H_2O_2 to samples without H_2O_2. Each sample measurement was replicated four times.

2.11. Markers of oxidative stress

a) **Plasma peroxides**

Endogenous plasma peroxides were analyzed with the Oxystat assay (a colorimetric assay, BI-5007, from Biomedica Medizinprodukte GmbH, Wien, Austria) according to the manufacturer's instructions. In this assay, endogenous plasma peroxides react with exogenously added peroxidase in the presence of the substrate 3,3′,5,5′-tetramethylbenzidine (TMB). In the presence of peroxides, the peroxidase oxidizes the TMB, producing a blue color. The reaction is stopped and stabilized by adding sulfuric acid, which converts the blue color to yellow. The intensity of the yellow signal is then measured spectrophotometrically at 450 nm, and the peroxide concentration is determined using a calibration curve.

Plasma was obtained by collecting blood in an EDTA tube, followed by centrifugation at 800 g for 10 minutes to separate plasma from RBCs. The plasma was then subjected to a second centrifugation at 5000 g for 5 minutes. Subsequently, peroxidase and TMB were added to the plasma to initiate the reaction. Each sample was analyzed in duplicate to ensure accuracy.

b) **Methemoglobin**

Following the collection of blood samples in EDTA tubes and centrifugation for 10 minutes at 800 g, 400 μL of RBCs were isolated and promptly frozen in liquid nitrogen. An original technique of low temperature electron paramagnetic resonance spectroscopy (EPR) to directly measure methemoglobin (MetHb) from the frozen samples was applied, using an EPR quartz finger Dewar filled with liquid nitrogen at 77 K, on a Bruker EMX100 X-band spectrometer with the following setting: microwave frequency, 9.35 GHz; modulation frequency, 100 kHz; microwave power, 20 mW; modulation amplitude, 7 mT; 7 scans [19].

c) **Myeloperoxidase activity**

Blood was collected in EDTA tubes and centrifuged at 800 g for 10 minutes to separate plasma, which was then promptly frozen at -80 °C. Myeloperoxidase activity was assessed by measuring the chlorination of tyrosine residues on proteins, specifically through the quantification of the ratio 3-chlorotyrosine/tyrosine bound-protein [26]. The reagents used for this assay are butanolic-HCl (3M) (87,472, from Merck) and hydrochloric acid (7647–01–0 from VWR), methanol LC-MS (10,675, 112, Fisher Scientific; phenol (W322318, Sigma-Aldrich). Sample preparation was performed as follows: 20 μL of plasma was deposited in each well, followed by the addition of 200 μL of 6N HCl. The microwave rotor was then filled with approximately 100 mL of 6N HCl containing 0.05 % phenol. Acid hydrolyzes was performed using a StartS microwave oven and a protein hydrolysis reactor (Milestone, Italy), which were carried out by heating to 110 °C over 5 min and maintaining the temperature at 110 °C for 30 min. The power was set at 800 W during the increase phase and 500 W to maintain the temperature. After cooling (30min), sample solutions were transferred from vials to 2 mL centrifugation tubes. Vials were washed with 300 μL methanol and solutions were dried under nitrogen. Dried samples were derivatized by butanolic-HCl at 60 °C for 15 min to obtain butyric esters of amino acids. Excess of butanolic-HCl was evaporated under nitrogen. The samples were diluted in 1mL formic acid 0.1 % and 10 μL were injected into LC–MS/MS.

LC-MS/MS analysis was conducted using an Agilent 6400 Series Triple Quadrupole LC/MS System (QqQ) coupled with an Agilent 1290 Infinity. Chromatographic separation was achieved on a Poroshell EC-120 C18 column (2.1 × 10 mm, 2.7 μm). The mobile phases consisted of 0.1 % formic acid in MilliQ water and pure methanol in gradient mode. The optimized transitions for chloro-tyrosine and tyrosine were acquired and the ratio of the area under the curve of chloro-tyrosine and tyrosine were obtained.

d) **MPO-dependent Oxidation of ApoA-1 and ApoB-100**

Blood was collected in EDTA tubes and centrifuged at 800g for 10 minutes to separate plasma, which was then promptly frozen at -80 °C. To assess the oxidation of these apolipoproteins, the degree of oxidation of two specific peptide residues from apolipoprotein A-1 (Tryptophan 72 -W72- and Methionine 148 -M148-) and two peptide residues from apolipoprotein B-100 (Tryptophan 1114 -W1114- and Methionine 4192 -M4192-) was analyzed.

The following reagents were used: Lipid Removal Agent (LRA) (PN 13,358-U, Sigma-Aldrich), 2,2,2-trifluoroethanol (PN 139,751,000, TFE, ACROS Organics), trypsin (PN T1426–250MG, Sigma-Aldrich), ammonium bicarbonate (PN 09830–500G, ABC, Sigma-Aldrich), dithiothreitol (PN D9779–5G, DTT, Sigma-Aldrich), iodoacetamide (PN I1149–5G, IAA, Sigma-Aldrich), and formic acid (PN 1.00264.0100,

Merck KGaA).

Plasma samples were prepared by adding 300 μL of 100 mM pH 8.0 ammonium bicarbonate (ABC) to 100 μL of plasma in a 2 mL Eppendorf Protein LoBind tube. Subsequently, 150 μL of LRA (100 mg/mL in ABC) was added, and the mixture was incubated at room temperature for 30 minutes with thermomixing. The samples were then centrifuged at 2200 g for 2 minutes, and the supernatant was removed, retaining the LRA pellets with lipoproteins. For protein reduction and alkylation, 50 μL of ABC, 50 μL of TFE, and 2 μL of DTT (31.0 mg/mL in MilliQ water) were added to the LRA pellets, followed by incubation at 60 °C for 1 h with thermomixing. After cooling to RT, 8 μL of IAA (37.0 mg/mL in MilliQ water) was added, and the mixture was incubated in the dark for 1 h at RT with thermomixing. Then, the samples were centrifuged again at 2200 g for 2 minutes, and the supernatant was removed. The LRA pellet was then incubated with 150.0 μL of MilliQ water, 50.0 μL of ABC, and 20.0 μL of trypsin (8.75 μg/μL) for 1 h at 37 °C with thermomixing. The reaction was quenched by adding 15.0 μL of 10 % formic acid. The mixture was centrifuged at 2200 g for 2 min, and the supernatant was collected for LC-MS/MS analysis. The LRA resin was washed with 150 μL of ABC, and the wash was also collected for analysis.

LC-MS/MS analysis was conducted using an Agilent 6400 Series Triple Quadrupole LC/MS System (QqQ) coupled with an Agilent 1290 Infinity. Chromatographic separation was achieved on a Poroshell EC-120 C18 column (2.1 × 10 mm, 2.7 μm). The mobile phases consisted of 0.1 % formic acid in MilliQ water and pure acetonitrile in gradient mode. The optimized transitions for the native peptides containing W72 and M148 on Apolipoprotein A1, as well as W1114 and M4192 on Apolipoprotein B100, and their corresponding oxidized forms, were acquired. These transitions reflect myeloperoxidase-dependent oxidation of HDL and LDL. The ratio of the area under the curve (AUC) for the oxidized versus native forms was calculated to assess the degree of oxidation.

2.12. Blood pressure assessment

Blood pressure was measured after a 5-minute rest period, with three consecutive readings taken. The final recorded value corresponded to the last measurement. Blood pressure was assessed using a cuff-based blood pressure monitor (Philips IntelliVue X2).

2.13. Assessment of adverse events

a) **Questionnaire evaluating adverse events**

Adverse events were evaluated using the Medical Dictionary for Regulatory Activities (MedDRA) terminology version 26. Volunteers received an online questionnaire containing common adverse events documented in the literature [27,28], such as abdominal cramps, excessive thirst, frequent bowel movements, nausea, and polyuria. Additionally, they were provided with a supplementary field to report any adverse events not listed. In cases where adverse events were not self-reported via the questionnaire, patients were contacted directly for further assessment.

b) **Routine biomarkers evaluating adverse events**

Routine clinical analyses were conducted at the laboratory of Cliniques Universitaires Saint Luc using standardized protocols. These analyses encompassed various parameters, including hepatic function markers (aspartate aminotransferase (ASAT), alanine aminotransferase (ALAT), gamma-glutamyl Transferase (GGT), markers of musculoskeletal health (lactate dehydrogenase (LDH) and creatine phosphokinase (CPK), renal function markers (creatinine, urea), complete blood count (hemogram including hemoglobin, hematocrit, platelets), ion levels (Ionogram including sodium, potassium and bicarbonate), lipid profile (lipogram including total-, LDL-, HDL-cholesterol and triglycerides), urinary sediment examination, and assessment of protein levels in urine (proteinuria).

2.14. Electronic data capture

Study data were collected and managed using REDCap electronic data capture tools hosted at Cliniques Universitaires Saint Luc. REDCap (Research Electronic Data Capture) is a secure, web-based software platform designed to support data capture for research studies, providing 1) an intuitive interface for validated data capture; 2) audit trails for tracking data manipulation and export procedures; 3) automated export procedures for seamless data downloads to common statistical packages; and 4) procedures for data integration and interoperability with external sources [29,30].

2.15. Statistical test used

Continuous variables were presented as means ± standard deviation (SD) or mean ± standard error of mean (SEM), while categorical variables were expressed as N and percentage.

Outliers were identified as values exceeding 2 SD and were subsequently excluded from the analysis.

Metabolite levels within groups were compared using the Friedman test or the Kruskal-Wallis test, followed by Dunn's post-hoc test for multiple comparisons, depending on the presence of outliers. Levels of metabolites between groups were analyzed using a mixed-effects model followed by a Sidak test for multiple comparisons.

To assess the blockade of AQP1 with purified Bacopaside II in RBCs on the time-dependent increase in fluorescence associated with the presence of ROS in RBCs (H_2-DCFDA test), we conducted a two-way ANOVA analysis followed by a Bonferroni post-hoc test.

To assess the impact of BM oral intake on the time-dependent increase in fluorescence associated with the presence of ROS in RBCs (H_2-DCFDA test), we conducted an ANOVA analysis, followed by a Tuckey test for multiple comparisons.

The antioxidant effect of metabolites in the plasma within groups was compared using a paired Wilcoxon matched pairs rank test, respectively for group A and B.

For other parameters such as MetHb, plasma peroxides, Cl-Tyr/Tyr, ox-HDL, ox-LDL and routine biomarkers, either a repeated measures one-way ANOVA or a Friedman test was employed, depending on the normality of the variables. Alternatively, we employed a Kruskal-Wallis test, followed by a Dunn's test for multiple comparisons when exclusion of outliers was needed. Hypothesis testing was two-tailed, and significance was determined at p-value < 0.05. The proportion of adverse events in the groups was analyzed using a chi-squared analysis. Data analysis was executed using Stata Statistical Software, StataCorp, College Station, Texas, Release 17 or GraphPad Prism version 10.0.0 for Windows, GraphPad Software, Boston, Massachusetts USA, www.graphpad.com.

3. Results

3.1. Description of groups

Twenty volunteers participated in the study, divided into two groups: Group A (n=10) received a daily dose of 400 mg of BM, while Group B (n=10) received 800 mg/d. Two participants from Group B (n=8) were excluded due to COVID-19 infection. The patient's study flow chart is shown in Fig. 2.

The mean ages were 40.9 ± 13.8 years and 44.5 ± 17.8 years for groups A and B, respectively. Both groups had an equal sex ratio of 1:1. The average BMI was 25.2 ± 5.4 kg/m^2 for group A and 24.4 ± 3.8 kg/m^2 for group B. The majority of volunteers were Caucasian, accounting for 80 % in group A and 100 % in group B. Only one participant in group A was an active smoker (10 %). Among female participants, 4 of them

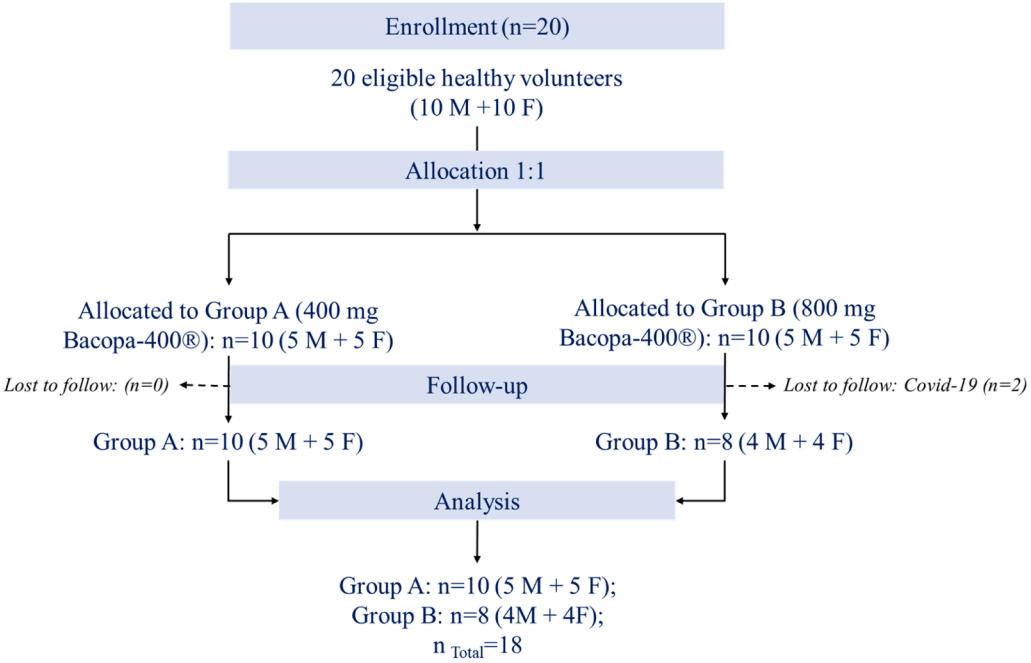

Fig. 2. Flowchart. M: Male; F: Female.

Table 3
Description of population.

	Group A (n=10)	Group B (n=8)	Total (n=18)
Age (y)	40.9 (13.8)	44.5 (17.8)	42.5 (15.3)
Sex ratio	1:1	1:1	1:1
Male (%)	5 (50)	4 (50)	
BMI (Kg/m²)	25.2 (5.4)	24.4 (3.8)	24.9 (4.6)
Ethnicity			
Caucasian (%)	8 (80)	8 (100)	16 (89)
African (%)	2 (20)	0 (0)	2 (11)
Smokers (%)	1 (10)	0 (0)	1 (5.5)
Medication or food supplement (%)	0 (0)	0 (0)	(0)
Method of contraception in female			
Contraceptive pill (% of female)	0 (0)	2 (50)	2 (23)
Hormonal intrauterine device (% of female)	1 (20)	1 (25)	2 (23)
Non-hormonal contraception (% of female)	3 (60)	0 (0)	3 (31)
Menopause (% of woman)	1 (20)	1 (25)	2 (23)
Compliance to BM treatment	9 (90)	8 (100)	17 (94)

BMI: body mass index

were using hormonal contraception (23 % oral contraceptive pill vs. 23% hormonal intrauterine device), 31 % were on non-hormonal contraception, and 23 % were menopausal. Table 3 provides an overview of the demographics of groups A and B. The compliance to the treatment was high, with only one volunteer in group A missing two doses during the V1 and V4 periods.

3.2. Detection of Bacopaside II in Bacopa-400® and its metabolites in plasma of healthy volunteers

a) Detection of Bacopaside II in Bacopa-400®

The content of Bacopaside II in BM extract was assessed via LC-MS-qTOF analysis. We used a standard of Bacopaside II (cf. Fig. 3a) in order to determine the retention time, the exact mass-to-charge ratio (*m/z*) of the ionized molecule and adducts, and the MS^E spectra obtained in low and high energy conditions. This investigation aimed to determine whether BM plant extract contained the specific AQP1-blocker. The extracted ion chromatogram of BM exhibited an identical peak matching with the retention time and MS^E spectra compared to the Bacopaside II standard, confirming the presence of Bacopaside II in the extract (cf. Fig. 3b), which was administered orally to healthy volunteers.

b) Identification of two putative Bacopaside II metabolites in the plasma of healthy volunteers following oral ingestion of Bacopa monnieri and molecular docking simulation on AQP1

Detection of Bacopaside II was examined in the plasma following oral ingestion of BM. No peak corresponding to Bacopaside II was identified in plasma samples from volunteers during the study (data not shown). We then conducted computational simulations to study the biotransformation processes of Bacopaside II. These processes include glucuronidation, glutathione S-conjugation, desaturation, reduction, oxidation, acetylation, and sulfation. Through this exploratory screening in plasma samples from volunteers, we identified several putative metabolites of Bacopaside II. A first group of isomeric metabolites characterized as the Bacopaside II aglycone with a SO_3 group and an oxygen atom, identified by a main peak at 6.85 minutes (Fig. 5a V4) was labeled "Metabolite 1″ ($C_{30}H_{48}O_8S$, $[M-H]^-$ 567.300, cf. Fig. 4b), while "Metabolite 2″ was identified as the Bacopaside II aglycone with a SO_3 group only ($C_{30}H_{48}O_7S$, $[M-H]^-$ 551.305, cf. Fig. 4c and Fig. 5b V4 at 9,65 minutes).

Notably, these metabolites were absent in chromatograms recorded from plasma at baseline (cf. Fig. 5a & 5b, V0). Following six weeks of BM intake (V4), chromatograms displayed the presence of both Metabolite 1 along with isomers sharing the same masse to charge ratio (*m/z*) (cf. Fig. 5a, V4), as well as Metabolite 2 (cf. Fig. 5b, V4). Moreover, these metabolites were no longer detectable four weeks after the end of treatment, as evidenced by the chromatograms in Fig. 5a & 5b, V6.

Quantitative detection of the Metabolites 1 and 2 signals was conducted upon normalization using the signal of added digitoxin used as internal standard.

Following treatment (V4), Metabolites 1 and 2 were observed in group A while being absent at baseline (Metabolite 1 V0: 0 a.u vs V4: 5 ± 2 a.u; $p<0.01$; cf. Blue Triangles Fig. 6 and Metabolite 2 V0: 0 a.u vs V4:

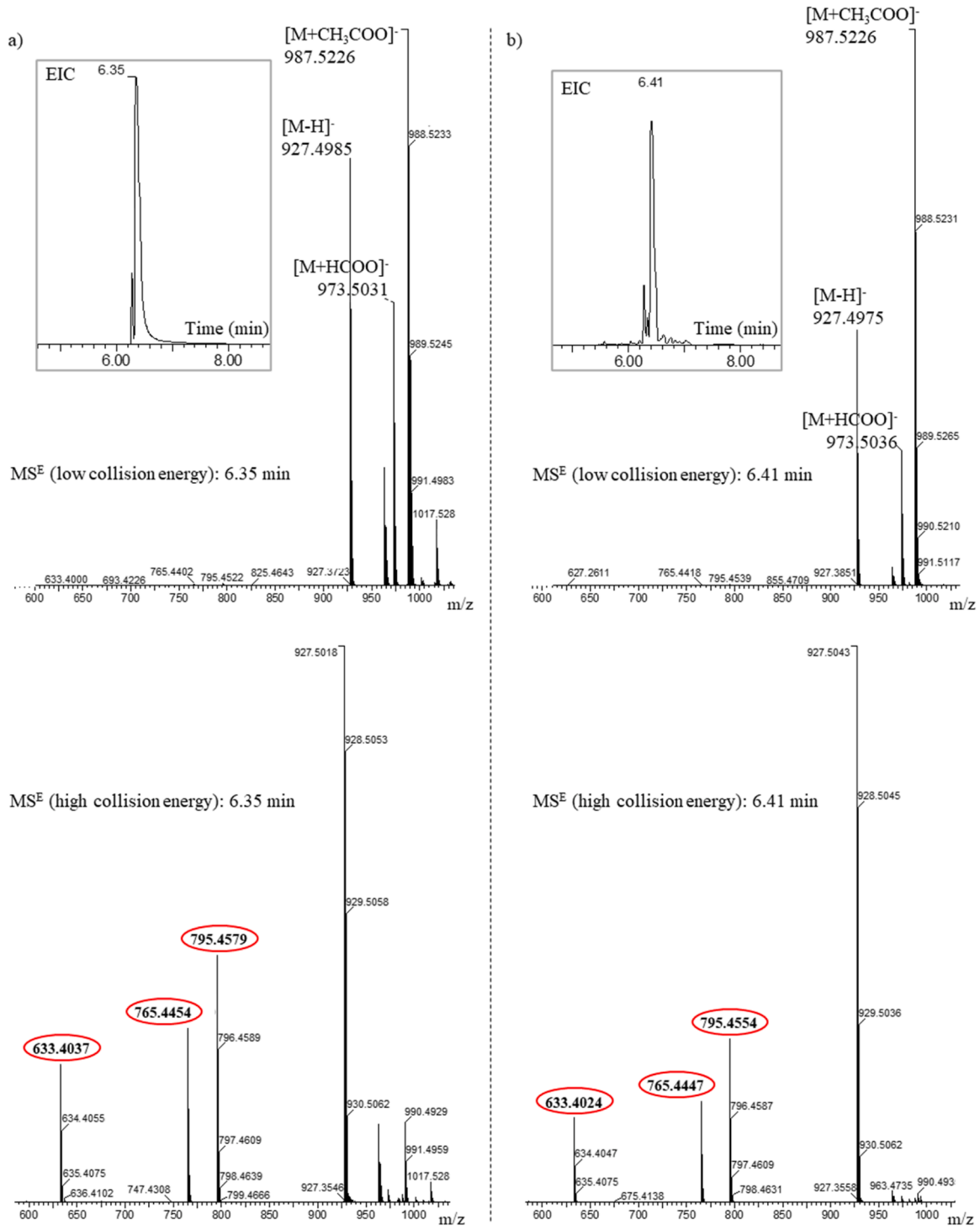

Fig. 3. Assessment of the presence of Bacopaside II in the Bacopa monnieri plant extract, Bacopa-400®. Extracted ion chromatograms EIC ($C_{47}H_{76}O_{18}$, $[M+CH3COO]^-$ 987.5170, ± 0.05 mDa) and mass spectra in MS^E (low and high collision energies) of the standard of Bacopaside II (Fig. 3a); and of the methanolic extract of Bacopa monnieri (Fig. 3b) containing Bacopaside II. Similar retention times (EICs) and adducts (MS^E low collision energy mass spectra) are observed. Similar patterns of fragmentation are highlighted (red circles) in MS^E (high collision energy mass spectra).

8 ± 2 a.u, $p<0.01$; cf. Orange Triangles Fig. 6). At V6 compared to V4, both Metabolite 1 and 2 levels decreased in group A (Metabolite 1 V4: 5 ± 2 a.u vs V6: 0 a.u; $p<0.001$; cf. Blue Triangles Fig. 6 and Metabolite 2 V4: 8 ± 2 a.u vs V6: 0 a.u, $p<0.0001$; cf. Orange Triangles Fig. 6).

A similar tendency was observed in group B with the presence of Metabolite 1 and 2 levels post-treatment (V4) while being absent at the baseline (Metabolite 1 V0: 0 a.u vs V4: 12 ± 4 a.u, $p<0.05$; cf. Blue Dots Fig. 6 and Metabolite 2 V0: 0 a.u vs V4: 29 ± 8 a.u, $p<0.05$; cf. Orange Dots Fig. 6). The levels of these two metabolites also significantly decreased at V6, compared to V4 in group B (Metabolite 1 at V4: 12 ± 4 a.u vs V6: 0, $p<0.001$; cf. Blue Dots Fig. 6 and Metabolite 2 V4: 29 ± 8 a.u vs V6: 0 a.u, $p<0.01$; cf. Orange Dots Fig. 6).

Additionally, at V4, the levels of Metabolites 1 and 2 were considerably higher in group B, in line with a higher intake of BM extract compared with Group A (Metabolite 1 group B V4: 12 ± 4 a.u vs group A V4: 5 ± 2 a.u; $p<0.01$, Blue Dots vs Blue Triangles Fig. 6; Metabolite 2

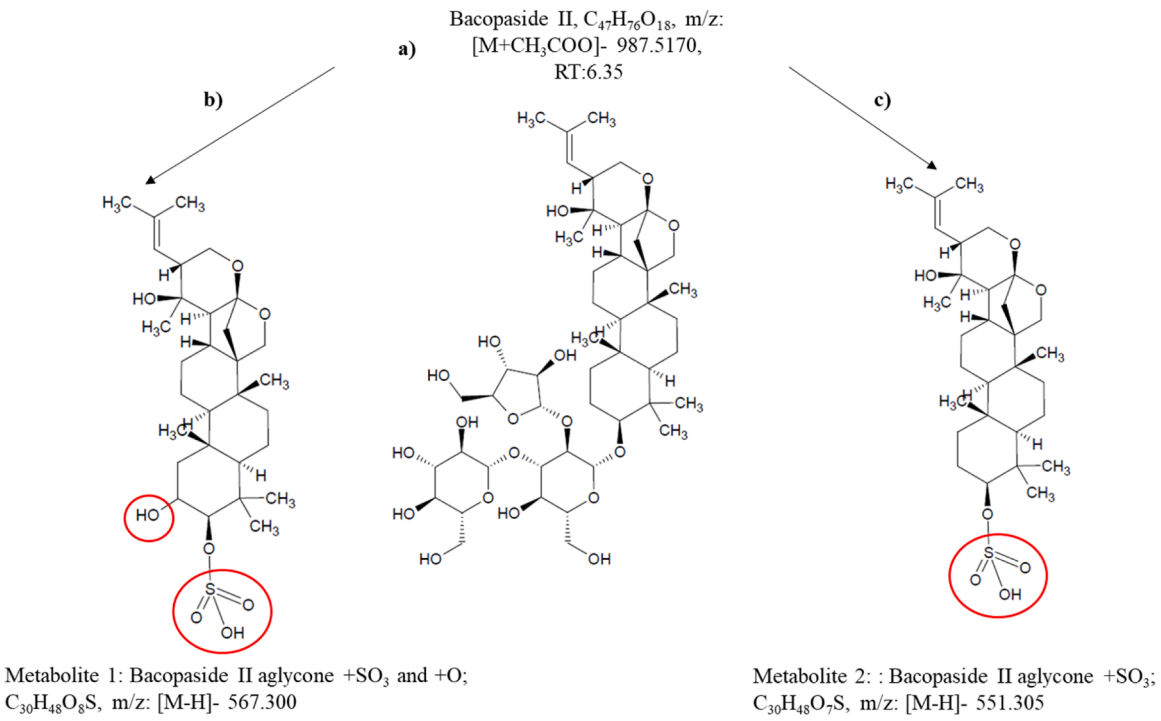

Fig. 4. Potential Metabolites Derived from Bacopaside II. Structure of the Bacopaside II ($C_{47}H_{76}O_{18}$) with a time of retention (RT) of 6.35 min and a mass-to-charge ratio (*m/z*) [M+CH3COO]$^-$ of 987.5 (Fig. 4a). Simulated structure of Metabolite 1 ($C_{30}H_{48}O_8S$) corresponding to the aglycone structure of Bacopaside II with the addition of SO_3 and one oxygen (Fig. 4b, the actual position of transformations in red circles remains unknown). The structure of Metabolite 2 ($C_{30}H_{48}O_7S$) corresponding to the aglycone structure of Bacopaside II with the addition of SO_3 (Fig. 4c, the actual position of transformations in red circles remains unknown). These metabolites were generated through simulation of biotransformation based on the structure of Bacopaside II.

group B V4: 29 ± 8 a.u vs group A V4: 8 ± 2 a.u, p<0.0001; Orange Dots vs Orange Triangles Fig. 6).

Molecular docking solutions of the two metabolites on AQP1 showed that they differ in their potential binding conformation on AQP1-intra subunit pore (cf. Fig 7c). The observed variation could possibly be due to the presence of a hydroxyl group in metabolite 1 (the exact position remaining unknown), which is absent in metabolite 2. The hydroxyl group in metabolite 1 appears to guide the SO_3 moiety into the pore of the AQP1 monomer, making the binding more energetically favorable. In contrast, the SO_3 moiety in metabolite 2, lacking the proximal hydroxyl group, remains outside the pore entrance, causing the compound to drift away from the channel opening and resulting in a less energetically favorable interaction.

3.3. Optimization of the H_2-DCFDA assay on red blood cells & assessment of Bacopaside II efficacy in blocking aquaporin I on red blood cell membranes

We conducted two experiments in order to validate our primary endpoint of assessing ROS levels in RBCs. We first aimed to determine the optimal concentration of the probe H_2-DCFDA. RBCs were loaded with varying concentrations of H_2-DCFDA ranging from 0 to 10 μM during 30 min. We selected the lowest effective concentration of H_2-DCFDA (1.5 μM) that produced a significant signal compared to the control (raw DCF MFI 0μM H_2-DCFDA=87 ± 9 a.u vs 1.5μM H_2-DCFDA = 959 ± 180 a.u, p<0.05; Supplementary Figure 1). Then RBCs were loaded with 1.5 μM of H_2-DCFDA and exposed to different concentrations of extracellular H_2O_2 (ranging from 0 to 50 μM, cf. Fig. 8a). As shown, H_2O_2 produced a time- and dose-dependent increase in the DCF signal. To stay close to physiological levels, we opted for the lowest concentration of H_2O_2 (10 μM) that induced a significant elevation of Dichlorofluorescein (DCF) mean fluorescence intensity (MFI) compared to the control (T31 min: standardized DCF MFI 0μM H_2O_2 = 39 ± 26 a.u vs 10 μM H_2O_2 = 469 ± 241 a.u, p<0.05; cf. Fig. 8a).

To assess the efficacy of Bacopaside II in blocking AQP1 on the membrane of RBCs, RBCs were incubated during 1 hour with Bacopaside II and subsequently loaded with H_2-DCFDA (1.5 μM) for 30 min; they were then exposed to 15 μM of H_2O_2, and the DCF signal was acquired over time. After incubation with Bacopaside II (10 μM), a significant decrease in standardized DCF MFI was observed compared to the control group (T25 min: standardized DCF MFI control = 1075 ± 212 a.u vs Bacopaside II = 636 ± 238 a.u, p < 0.05; cf. Fig. 8b).

3.4. Effect of oral intake of Bacopa monnieri extracts, containing the AQP1-blocker, Bacopaside II, on systemic oxidative stress of healthy volunteers

a) Assessment of ROS levels in RBCs before and after Bacopa monnieri treatment in healthy volunteers

To assess the effect of BM extracts in healthy volunteers at baseline (V0), after 6 weeks of BM treatment (V4) and 4 weeks after the end of the treatment (V6), RBCs were loaded with H_2-DCFDA and subsequently exposed to extracellular H_2O_2. The resulting fluorescence intensity of DCF was quantified using FACS and represented as Standardized DCF MFI according to time. We pooled the standardized DCF MFI of group A and B at V0 (n=18), next the standardized DCF MFI were compared between groups at subsequent visits. The analysis showed a significant effect of time (p < 0.001, cf. Fig. 9a-9d), indicating variations in standardized DCF MFI over the 40-minute period. There was also a significant main effect of visit groups (p < 0.001, cf. Fig. 9a-9d), revealing differences in standardized DCF MFI across the various visits and groups (A vs. B). Additionally, a significant main effect of subjects (p < 0.001, cf. Fig. 9a-d) was observed, indicating variations in standardized DCF MFI between individual subjects of the study. After 6 weeks of daily oral intake of BM extracts, the standardized DCF MFI tended to decrease in group A (T40 min: Standardized DCF MFI V0=381 ± 43 a.u vs V4= 362 ± 42 a.u, p=ns; cf. Fig. 9a & Supplementary Table 3), while in group B, a

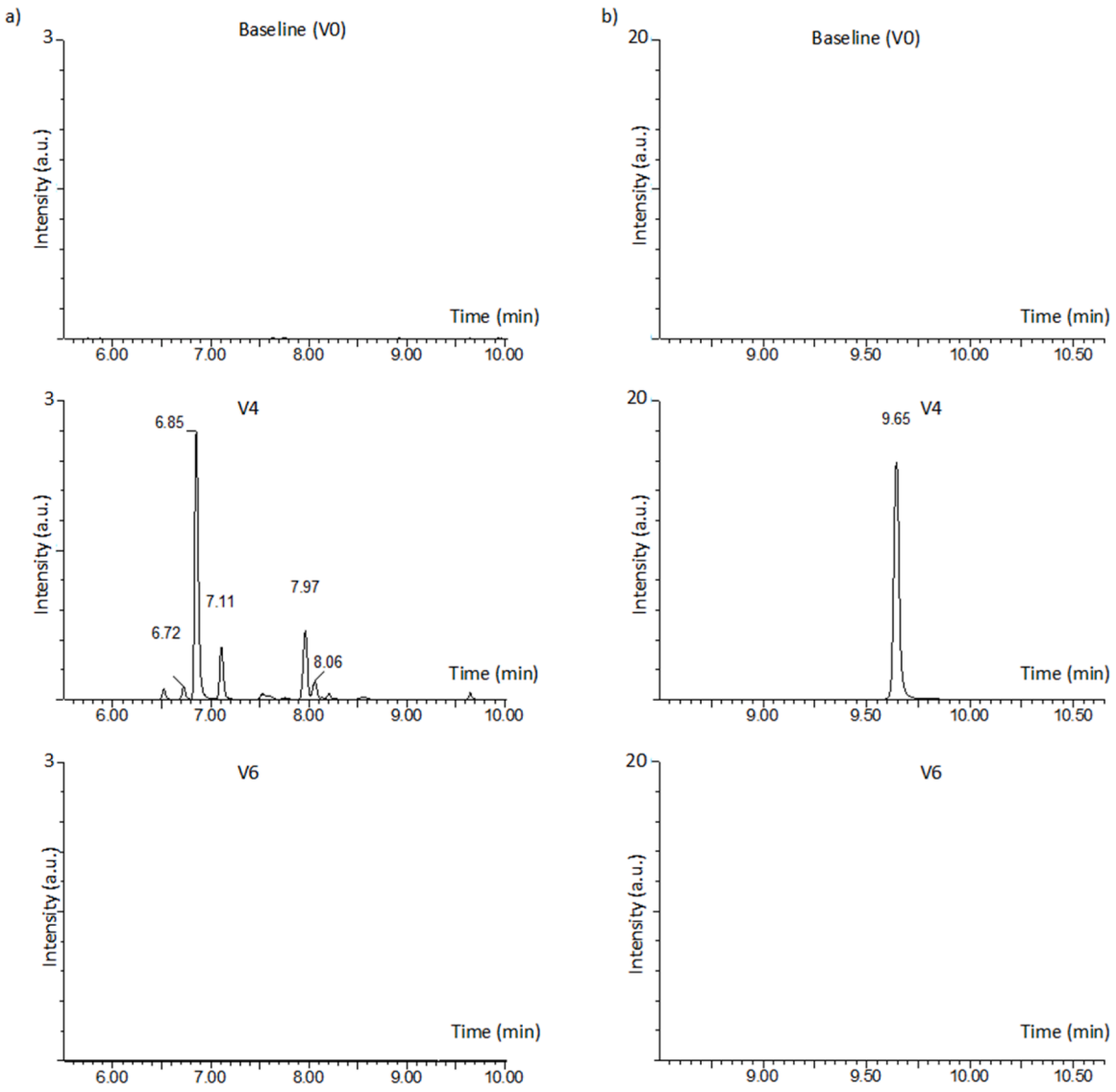

Fig. 5. Detection of putative metabolites of Bacopaside II in the plasma of healthy volunteers along the study. Extracted ion chromatograms (MS^E low collision energy) of Metabolite 1 and isomers at different time points (V0, V4 and V6): $C_{30}H_{48}O_8S$, $[M-H]^-$ 567.300, ± 5 mDa (Fig. 5a). Extracted ion chromatograms (MS^E low collision energy) of Metabolite 2 at different time points (V0, V4, and V6): $C_{30}H_{48}O_7S$, $[M-H]^-$ 551.305, ± 5 mDa (Fig. 5b). a.u. arbitrary units. These chromatograms are representative of one volunteer from group B. However, this analysis was performed on all 18 volunteers who completed the study.

significant decrease in standardized DCF MFI was observed (T40 min: Standardized DCF MFI V0=381 ± 43 a.u vs V4= 187 ± 69 a.u, p<0.01; cf. Fig. 9c & Supplementary Table 3). This effect was reversible, with standardized DCF MFI returning to baseline levels 4 weeks after the end of treatment for both, group A (T40 min: Standardized DCF MFI V6=372 ± 54, p=ns; cf. Fig. 9b & Supplementary Table 3) and group B (T40 min: Standardized DCF MFI V6=339 ± 36 a.u, p=ns; cf. Fig. 9d & Supplementary Table 3).

b) **Bacopa Monnieri components in plasma have no antioxidant activity *per se***

The potential antioxidant effects of BM components in plasma were assessed. No significant difference was observed in the Amplex-red response after adding 200 μM of H_2O_2 in the plasma at V0 and V4 in either group A (V0 = 9.9 ± 1.0 a.u vs. V4 = 9.4 ± 1.3 a.u; p = ns; cf. Fig. 10a) or group B (V0 = 9.4 ± 1.0 a.u vs. V4 = 9.1 ± 1.4 a.u; p = ns, cf. Fig. 10b).

c) **Assessment of markers of systemic oxidative stress before and after Bacopa monnieri treatment in healthy volunteers**

The measurements of plasma peroxides (PP), reflecting oxidative stress were performed in each group of treatment. In group A, there was no difference in PP levels after 6 weeks of oral BM treatment (PP V0 = 549.6 ± 121.1 μM vs PP V4: 566.1 ± 98.5 μM; p=ns, cf. Fig. 11a) whereas a non-significant decrease was observed in group B (PP V0= 386.2 ± 80.5 μM vs PP V4= 352.0 ± 38.7 μM; p=ns, cf. Fig. 11c).

Methemoglobin (MetHb) concentrations in RBCs, another specific marker of oxidative stress, were reduced under BM treatment. In group A, MetHb levels decreased after 6 weeks of BM treatment (MetHb V0: 0.64 ± 0.06 a.u vs MetHb V4: 0.26 ± 0.04 a.u; p<0.001, cf. Fig. 11b) and this reduction remained significant even 4 weeks after the end of treatment (MetHb V0: 0.643 ± 0.065 a.u vs V6: 0.183 ± 0.080 a.u, p<0.001, cf. Fig. 11b). A similar significant decrease was observed in group B at V4 (MetHb V0: 0.900 ± 0.105 a.u vs MetHb V4: 0.233 ± 0.047 a.u; p<0.001, cf. Fig. 11d) and this effect was maintained at V6 (MetHb V0: 0.900 ± 0.105 a.u vs MetHb V6: 0.166 ± 0.042 a.u, p<0.0001, cf. Fig. 11d).

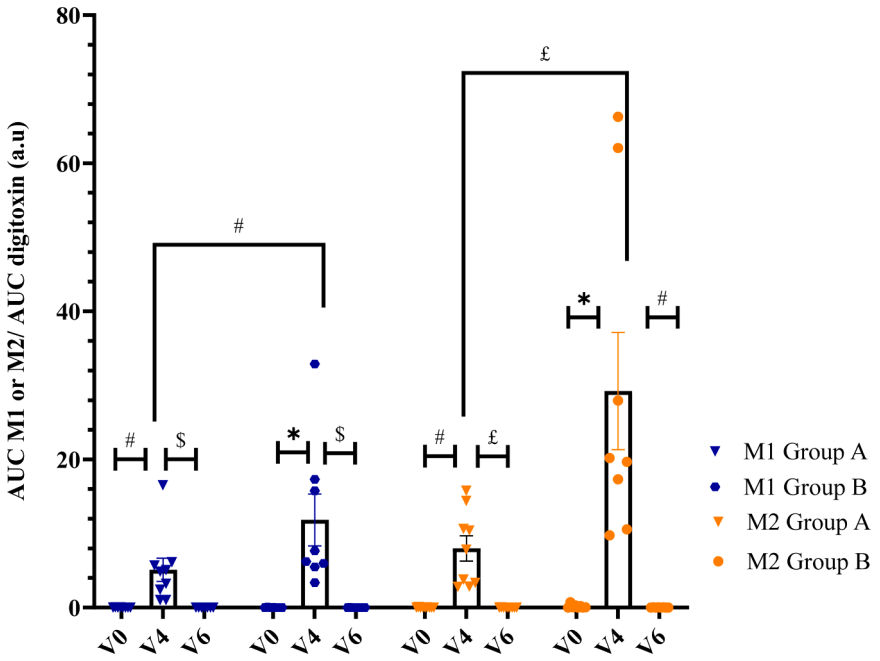

Fig. 6. Comparative levels of the putative metabolites derived from the Bacopaside II in the plasma of heathy volunteers after 6 weeks of daily oral intake of Bacopa monnieri. Comparative levels of **Metabolite 1 (M1)** at V0 (n=8), V4 (n=9) and V6 (n=7) in **group A (Blue Triangles)**; #p<0.01, $p<0.001; Data were represented as mean and SEM and were submitted to a Kruskal-Wallis test, followed by a Dunn's test for multiple comparisons. In group A, 6 outliers (>2 SD) were removed (2 at V0, 1 at V4, and 3 at V6). Comparative levels of **M1** at V0 (n=7), V4 (n=8), and V6 (n=8) in **group B (Blue Dots)**; *p<0.05, $p<0.001; Data were represented as mean and SEM and were submitted to a Kruskal-Wallis test, followed by a Dunn's test for multiple comparisons. In group B, 1 outlier (>2 SD) was removed at V0. Comparative levels of **Metabolite 2 (M2)** at V0 (n=9), V4 (n=9), and V6 (n=10) in **group A (Orange Triangles)**. *p<0.05, #p<0.01, £p<0.0001; Data were represented as mean and SEM and were submitted to a Kruskal-Wallis test, followed by a Dunn's test for multiple comparisons. In group A, 2 outliers were removed (>2 SD) (1 at V0 and 1 at V4). Comparative levels of **M2** at V0 (n=8), V4 (n=8), and V6 (n=8) in **group B (Orange Dots)**. *p<0.05, $p<0.001; Data were represented as mean and SEM and were submitted to a Fridman test, followed by a Dunn's test for multiple comparisons. Levels of M1 at V4 in group A (n=9; Blue Triangles) vs. B (n=8; Blue Dots) were assessed by a mixed-effect analysis, followed by a Sidak test for multiple comparisons; #p<0.01. Levels of M2 at V4 in group A (n=9; Orange Triangles) vs. B (n=8; Orange Dots) were assessed by mixed-effect analysis, followed by a Sidak test for multiple comparisons; £p<0.001.

The effects of BM intake on MPO activity products were also investigated. In Group A, the 3-chlorotyrosine/tyrosine (Cl-Tyr/Tyr) ratio exhibited a decreasing trend, though it was not statistically significant at V4 (Cl-Tyr/Tyr V4: $6.3 \times 10^{-5} \pm 1.3 \times 10^{-5}$ a.u.; p=ns, Fig. 12a) compared to V0 (Cl-Tyr/Tyr V0: $9.1 \times 10^{-5} \pm 1.6 \times 10^{-5}$ a.u; Fig. 12a). However, the decrease was significant at V6 (Cl-Tyr/Tyr V6: $5.1 \times 10^{-5} \pm 0.83 \times 10^{-5}$ a.u.; p<0.05; Fig. 12a) compared to V0. A similar trend was observed in Group B even though it was not statistically significant (Cl-Tyr/Tyr V0: $5.0 \times 10^{-5} \pm 0.88 \times 10^{-5}$ a.u.; V4: $4.3 \times 10^{-5} \pm 0.78 \times 10^{-5}$ a.u.; V6: $3.6 \times 10^{-5} \pm 0.54 \times 10^{-5}$ a.u.; p=ns, Fig. 12c).

To monitor the oxidation of High-Density Lipoproteins Cholesterol (HDL), the degree of oxidation of two peptide residues from Apolipoprotein A-1 (ApoA-1), Methionine 148 (ratio M148-ox/M148) and Tryptophan 72 (ratio W72-ox/W72) was assessed. In Group A, a significant decrease in the M148-ox/M148 ratio was observed at V4 (0.02 ± 0.00 a.u.; p<0.05, Fig. 12b) compared to V0 (0.10 ± 0.02 a.u., Fig. 12b) and this effect persisted at V6 (0.01 ± 0.00 a.u.; p<0.001, Fig. 12b). Similarly, in Group B, the M148-ox/M148 ratio significantly decreased at V4 (0.02 ± 0.00 a.u.; p<0.05, Fig. 12d) compared to V0 (0.06 ± 0.01 a.u., Fig. 12d) and this effect persisted at V6 (0.01 ± 0.00 a.u.; p<0.001, Fig. 12d).

No significant differences were observed in the degree of oxidation of the W72 peptide residue after treatment (Tables 5&6). Additionally, the degree of oxidation of Tryptophan 1114 (ratio W1114-ox/W1114) and Methionine 4192 (ratio M4192-ox/M4192) residues of the Apolipoprotein B-100 (ApoB-100) of Low-Density Lipoproteins Cholesterol (LDL) showed no significant change before or after treatment in either Group A or Group B (Tables 5& 6).

3.5. Impact of ROS reduction on blood pressure in healthy volunteers

We investigated the effect of oral intake of BM extracts on blood pressure. In group A, we observed a slight but non-significant decrease of systolic blood pressure (SBP) after 6 weeks of BM treatment (Group A: SBP V0: 131 ± 20 mmHg vs SBP V4: 127 ± 11 mmHg, p=ns, cf. Fig. 13a). Administering a higher dose of BM extracts (group B) resulted in a significant reduction in systolic blood pressure by the end of the treatment period (Group B: SBP V0=131 ± 15 mmHg vs SBP V4=116 ± 7 mmHg; p < 0.05, cf. Fig. 13d). There was also a significant decrease in mean blood pressure at higher concentration (Group B: MBP V0= 98 ± 8 mmHg vs MBP V4: 89 ± 7 mmHg; p < 0.01, cf. Fig. 13f). Furthermore, this effect on MBP persisted 4 weeks after the cessation of treatment (Group B: MBP V0= 98 ± 8 mmHg vs MBP V6= 88 ± 10 mmHg; p < 0.05, cf. Fig. 13f).

3.6. Oral intake of Bacopa monnieri is safe

Following the initiation of the treatment, volunteers were monitored to document adverse events (AE), as detailed in Table 4. Reported AE mirrored those commonly described in the literature, including abdominal cramps (20 % in group A and 62.5 % in group B), excessive thirst (10 % in group A), polyuria (25 % in group B), and nausea (10 % in group A and 12.5 % in group B). The only unexpected AE reported was muscular pain after 3 weeks of treatment. It was observed that volunteers in the group B experienced a higher incidence of AE compared to those in group A (87.5 % and 30 % incidence, respectively (p < 0.001). No serious adverse events were observed, and no volunteers discontinued the study due to treatment-related difficulties.

In terms of laboratory values, no clinically relevant differences were

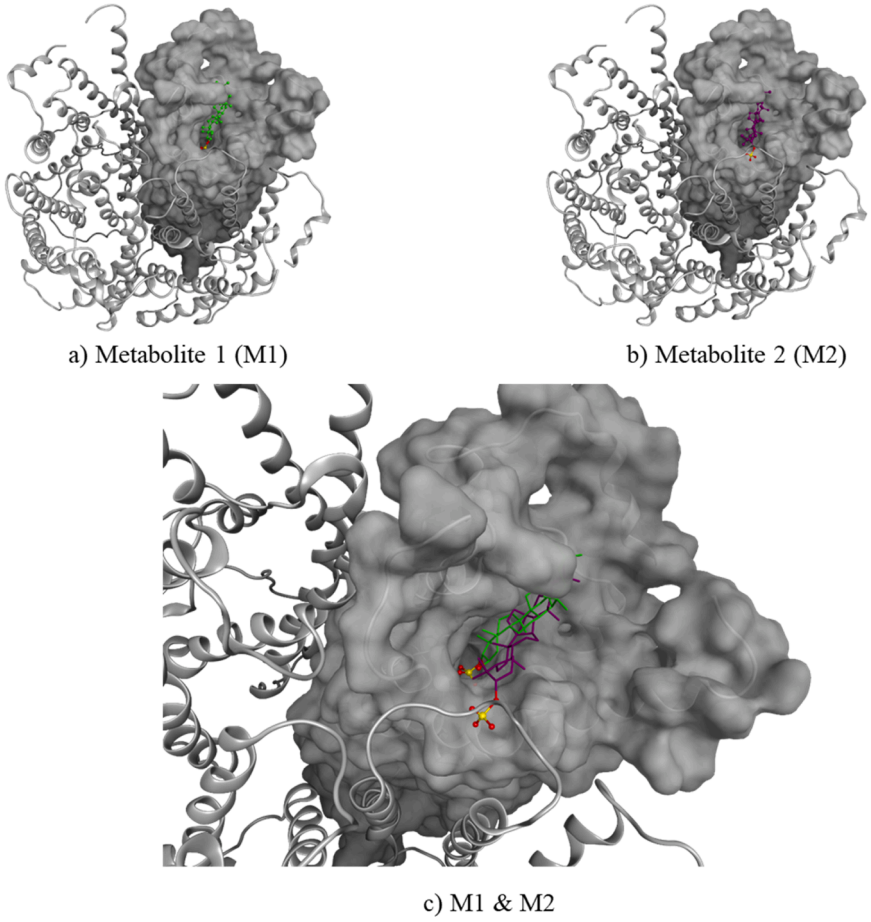

Fig. 7. Putative Docking sites of Bacopaside II metabolites on AQP1. Theoretical binding poses adopted by metabolite 1 (Fig. 7a) and metabolite 2 (Fig. 7b) on an AQP1 intra-subunit pore. AQP1 is depicted as a grey cartoon with a monomer presented as a grey molecular surface. Metabolite 1 (green) and metabolite 2 (purple) are shown in ball-and-stick representation, with oxygen atoms in red and sulfur atoms in yellow. A magnified view of the binding sites highlights the differences in the binding conformation of the two metabolites on the AQP1 monomeric pore (Fig. 7c). Metabolite 1 appears to bind deeper within the pore, guided by the proximity of its SO_3 group and a hydroxyl group, resulting in a more energetically favorable interaction. In contrast, metabolite 2, which lacks the proximal hydroxyl group, seems to drift away from the channel, with its SO_3 moiety sticking out of the pore, suggesting a less energetically favorable interaction.

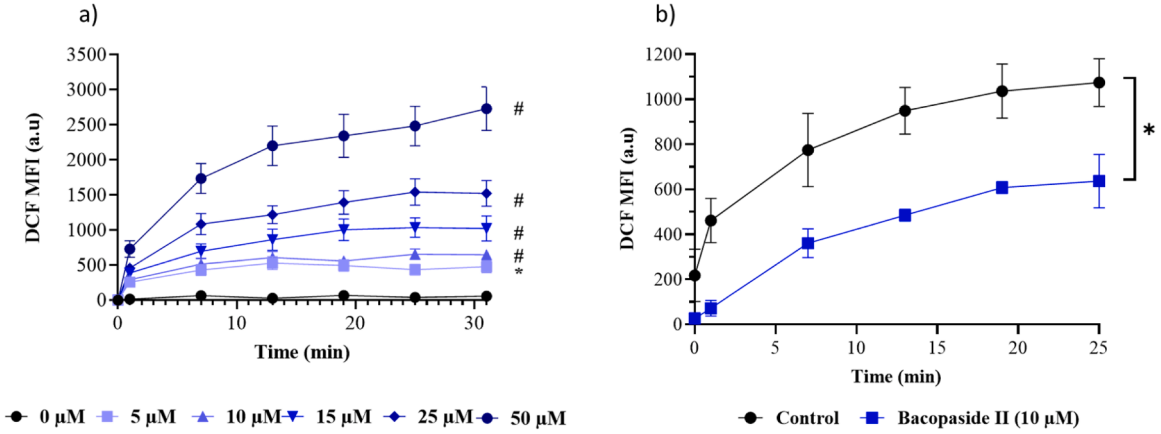

Fig. 8. Time- and concentration-dependent effects of H_2O_2 on standardized DCF MFI in human erythrocytes (Fig. 8a). Comparative time-dependent increase in standardized DCF MFI of RBCs loaded with the chosen concentration of 1.5 µM of H_2-DCFDA, following exposure to increased concentrations of extracellular H_2O_2. The time-dependent increase in fluorescence was monitored over a 31-minute period (after 1 min then each 6 minutes up to 31 minutes). The effect of the different concentrations of extracellular H_2O_2 were compared to the control (without H_2O_2). n= 5 volunteers. *p<0.05, #p<0.01; compared to control. Data were represented as mean and SEM and subjected to a two-way ANOVA followed by a Bonferroni post hoc test. **Inhibitory effect of Bacopaside II, a specific blocker of water channel aquaporin 1 (AQP1), on H_2O_2-induced intracellular standardized DCF MFI in human erythrocytes** (Fig. 8b). Comparative increase in intracellular reactive oxidant species (ROS; measured by DCF fluorescence) over time in RBCs incubated with or without 10 µM of Bacopaside II and exposed to extracellular 15 µM of H_2O_2. Standardized DCF MFI comparison of RBCs incubated or not (control) with Bacopaside II; n 4 volunteers. *p<0.05. Data were represented as mean and SEM and subjected to a two-way ANOVA followed by a Bonferroni post-hoc test.

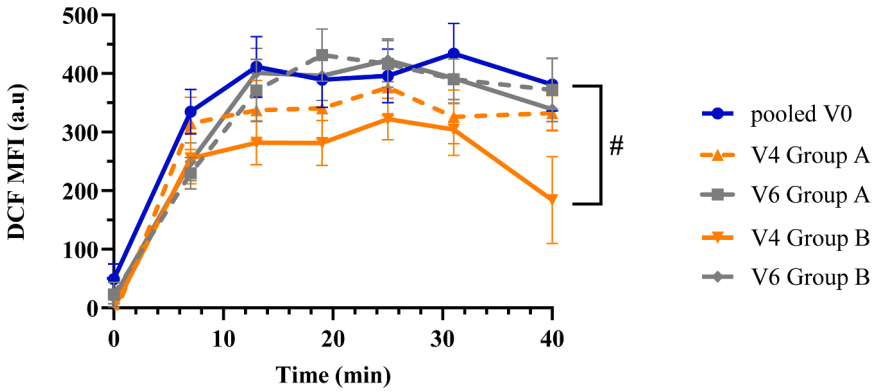

Fig. 9. A chronic oral administration of Bacopa monnieri extract dose-dependently decreases the reactive oxygen species (ROS) detection into red blood cells (RBCs) measured by DCF fluorescence: Comparative increase in standardized DCF MFI over time in RBCs exposed to extracellular H_2O_2. Standardized DCF MFI comparison between pooled V0 (n=18) and V4 Group A (n=10; solid orange line) and between pooled V0 (n=18) and V6 Group A (n=10; solid grey line); Standardized DCF MFI comparison between pooled V0 (n=18) and V4 Group B (n=8; dotted orange line) and between pooled V0 (n=18) and V6 Group B (n=8; dotted grey line). The time-dependent increase in standardized DCF MFI was measured over a period of 40 minutes. #p<0.01 compared to pooled V0; Data were represented as mean and SEM and subjected to an ANOVA analysis including standardized DCF MFI as the dependent variable and time (0–40 min), visit groups (pooled V0, V4 Group A, V4 Group B, V6 Group A, V6 Group B), and subjects as independent variables, followed by a Tukey test for multiple comparisons. The results showed a main effect of time (p<0.001), visit groups (p<0.001) and subjects (p<0.001).

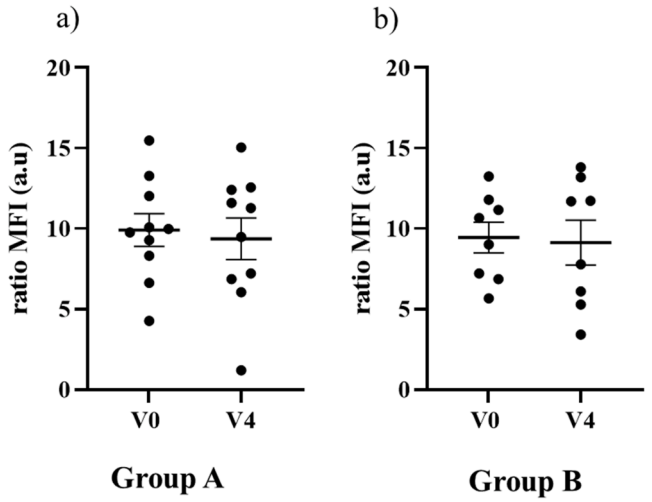

Fig. 10. Assessment of the antioxidant effects of Bacopa monnieri extracts in plasma. Amplex-red response was measured after the addition of 200 μM H_2O_2 in the plasma samples obtained at baseline (V0) and after 6 weeks of Bacopa monnieri treatment (V4) in groups A (Fig. 10a) and B (Fig. 10b). n Group A =10 and n Group B=8. Data are presented as mean and SEM and submitted to a paired Wilcoxon matched-pairs rank test.

observed in hepatic function markers (AST, ALT, GGT), renal function markers (creatinine, urea, GFR), blood cell counts (hemoglobin, hematocrit, platelets), or ionogram values (Tables 5 & 6). After 6 weeks of BM intake, an increase in LDL-cholesterol levels was observed in group A (V0: 104.2 ± 38.8 to V4: 122.1 ± 47.4 mg/dL; $p < 0.05$, cf. Fig. 14b) and group B (V0: 132.2 ± 29.7 to V4: 157.0 ± 45.1 mg/dL; $p < 0.05$, cf. Fig. 14e). Nevertheless, this increase fully reversed by the end of the treatment period in group A (from V0: 104.2 ± 38.8 to V6: 115.6 ± 40.5 mg/dL; p = ns, cf. Fig. 14b) and group B (from V0: 132.2 ± 29.7 to V6: 137.6 ± 29.0 mg/dL; p = ns, cf. Fig. 14e).

In Group B, the lipid profile evolution included total cholesterol (nV0=8, nV2=8, nV4=8 and nV6=8; Fig. 14d), LDL-cholesterol (nV0=8, nV2=8, nV4=8 and nV6=8; Fig. 14e) and triglycerides (nV0=8, nV2=7, nV4=8 and nV6=8; Fig. 14f); *p<0.5. Data were also presented as boxplots. Statistical comparisons for total cholesterol and LDL-cholesterol were conducted using the repeated measures Friedman test followed by a Dunn's test for multiple comparisons. Triglycerides were analyzed using the Kruskal-Wallis test. One outlier (>2SD) was excluded at V2 for triglycerides.

4. Discussion

In this interventional study on healthy volunteers, the main effects of oral supplementation with Bacopa monnieri (BM) extracts can be summarized as follows: i. reduction in intracellular ROS accumulation within RBCs exposed to extracellular H_2O_2; ii. no direct ROS scavenging effect of BM derivatives in plasma; iii. reduction levels of Methemoglobin (MetHb) and oxidized apolipoprotein A-1 of HDL (M148-ox/M148) indicating reduced systemic oxidative stress; iv. reduction in blood pressure profile at higher dosage. Two Bacopaside II metabolites (and their putative binding sites on human AQP1) were identified in plasma under BM oral intake, which were cleared four weeks post-treatment. Monitoring of clinical chemistry values confirmed the safety of daily intake of BM (up to 800 mg/day) for 6 weeks.

Preventing cardiovascular diseases is an important public health challenge. Specifically, targeting endothelial function is crucial because it plays a central role in the initiation of atherosclerosis. Endothelial dysfunction *per se* is a reversible phenomenon and its improvement may be achieved by eliminating cardiovascular risk factors under healthy lifestyle modifications, encompassing dietary adjustments and regular exercise [31]. Pharmacological interventions, such as drugs antagonizing vascular pro-oxidant or vasoconstrictor pathways (e.g., Angiotensin-converting enzyme inhibitors, angiotensin II receptor antagonists, calcium channel blockers), or cholesterol-lowering therapies (i.e., statins), offer additional avenues for improvement [32–34]. Nevertheless, these medications are typically prescribed to individuals already afflicted with conditions such as high blood pressure, diabetes, hypercholesterolemia, or other cardiovascular diseases, as they exert a protective effect on the endothelium tailored to the specific underlying mechanisms of endothelial dysfunction [35].

Moreover, the administration of exogenous antioxidants, such as vitamins E, C, and beta-carotene, has not demonstrated efficacy in reducing atherosclerosis, as evidenced by findings from several meta-analyses [36–40]. This lack of success may be attributed to several factors, including uncertainties surrounding the bioavailability of synthetic antioxidants and the determination of their optimal dosing further complicates their therapeutic application [41]. Although specific treatments targeting NOS-dependent endothelial dysfunction, such as

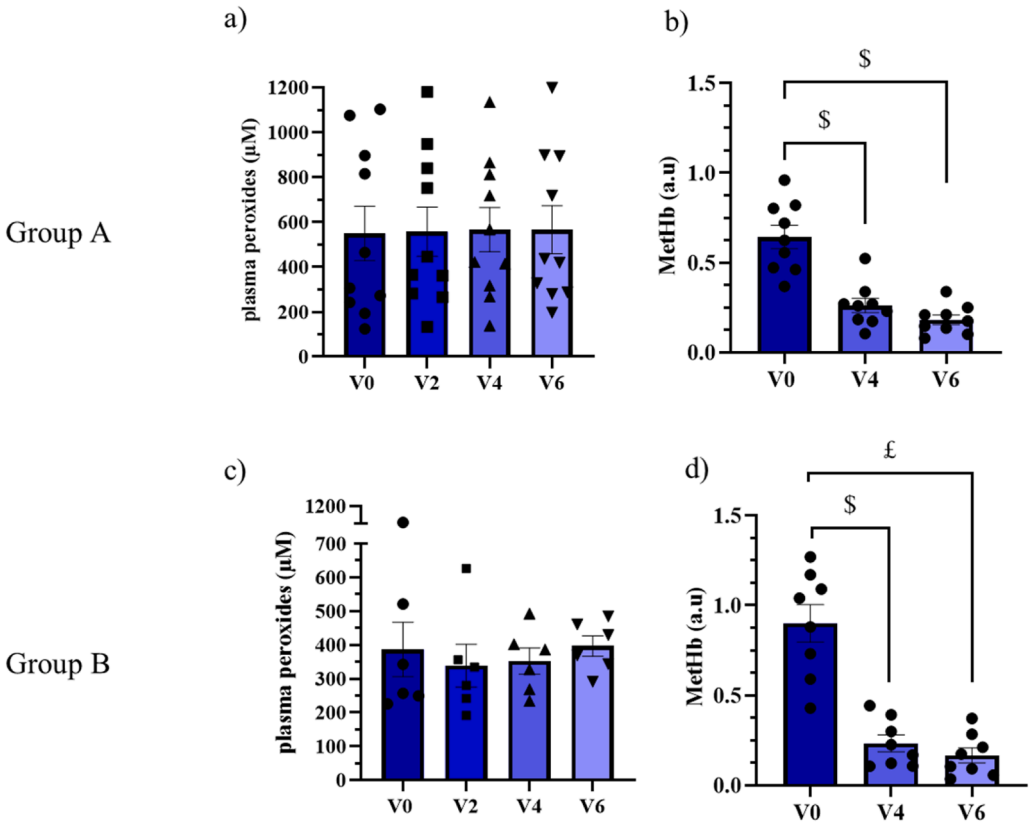

Fig. 11. Changes in plasma peroxides and methemoglobin (MetHb) levels after 6 weeks of daily oral intake of Bacopa monnieri. In **group A (400 mg/d)** evolution of **plasma peroxides** (Fig. 11a) at V0 (n=10), V2 (n=10), V4 (n=10) and V6 (n=10) and MetHb (Fig. 11b) at V0 (n=10), V4 (n=10) and V6 (n=10); $p<0.005; £p<0.001. Data were represented as mean and SEM and were subjected to a repeated measures one-way ANOVA, followed by a Bonferroni post-hoc test. In group B (800 mg/d) evolution of plasma peroxides (Fig. 11c) at V0 (n=6), V2 (n=6), V4 (n=6) and V6 (n=8) and MetHb (Fig. 11d) at V0 (n=8), V4 (n=8), V6 (n=8); $p<0.001; £p<0.0001 compared to V0. Data were represented as mean and SEM. Plasma peroxides were submitted to a Kruskal Wallis, followed by a Dunn's test for multiple comparisons and MetHb were subjected to a repeated measures one-way ANOVA, followed by a Bonferroni post-hoc test. 8 outliers (>2SD) were removed in Fig. 11c (2 at V0, V2, V4 and V6 respectively).

L-arginine or tetrahydrobiopterin (BH_4) supplementation, were previously considered, their efficacy is limited due to impaired NOS function, resulting from the prevailing endothelial oxidant stress and NOS uncoupling [42]. In this context, modulating the activity of AQP1 as a 'peroxiporin' to regulate the entry of ROS into endothelial cells, using a targeted inhibitor, could represent a promising new therapeutic strategy to restore the redox balance in the endothelium and increase the bioavailability of NO.

Bacopaside II is recognized for its ability to selectively block the AQP1 water channel [17]. We previously confirmed the potential of BM extracts, containing Bacopaside II, to inhibit the water channel of human AQP1 monomers expressed in modified Xenopus oocytes [16]. Our current results are in line with this paradigm by demonstrating the efficacy of Bacopaside II to decrease ROS levels within RBCs following exposure to extracellular H_2O_2. We used RBCs as indicators of the AQP1-mediated oxidative stress because these cells express large amounts of plasmalemmal AQP1, primarily responsible for erythrocyte volume changes in response to environmental tonicity [21] and possess an extensive antioxidant system linked to continuous exposure to endogenous and exogenous sources of ROS [43]. Accordingly, oxidative stress-related erythropathies are proposed as "surrogates" to monitor the development of cardiovascular diseases because they reflect the vascular redox status [44]. Notably, angiotensin II (Ang II)-dependent oxidative stress directly contributes to the senescence of erythrocytes and their susceptibility to eryptosis [45].

Although we cannot directly prove the causality of AQP1 blockade in the antioxidant protection after oral BM intake, our observations are in line with our previous report, which demonstrated an attenuation of the DCFDA fluorescent signal upon exposure of *Aqp1* KO cardiac myocytes to extracellular H_2O_2 (compared to WT). In the latter study, we definitively identified H_2O_2 as the specific oxidant species transported by AQP1 by using a Hyper3 fluorescent reporter specific for H_2O_2 fused to a peptide targeting caveolae on the myocyte membrane [16]. We also proposed putative binding sites of Bacopaside II on the cytoplasmic side of the AQP1 monomeric pore, which are, in part, recapitulated in our present simulations with the 2 identified plasma metabolites of BM. The absence of detectable chemical antioxidant effect of these or other components in the plasma (by Amplex Red assay) further reinforces the probability of a specific interaction with AQP1.

The attenuation of ROS levels in RBCs after oral intake of BM was paralleled with an improvement of specific biomarkers linked to oxidative stress. MetHb is the oxidized form of hemoglobin resulting from the action of ROS, including H_2O_2, reflecting the imbalanced antioxidant system in RBCs [46]. In turn, MetHb can produce large quantities of free radicals involved in the oxidation of lipoproteins and the release of heme into the bloodstream, which are implicated in oxidative tissue damage, leading to a vicious circle [47]. MetHb is therefore not only a marker of RBCs oxidative stress but also participates to the atherosclerosis-related inflammation [48]. Our present observations indicated that 6-week oral supplementation with BM extract in healthy volunteers was sufficient to induce significant reductions in MetHb levels, which persisted even four weeks after the treatment was discontinued.

In the vasculature, MPO is a heme-containing enzyme that uses extracellular H_2O_2, generated primarily through the activation of (Nox)-2, along with chloride ions to produce the powerful halogenous oxidant

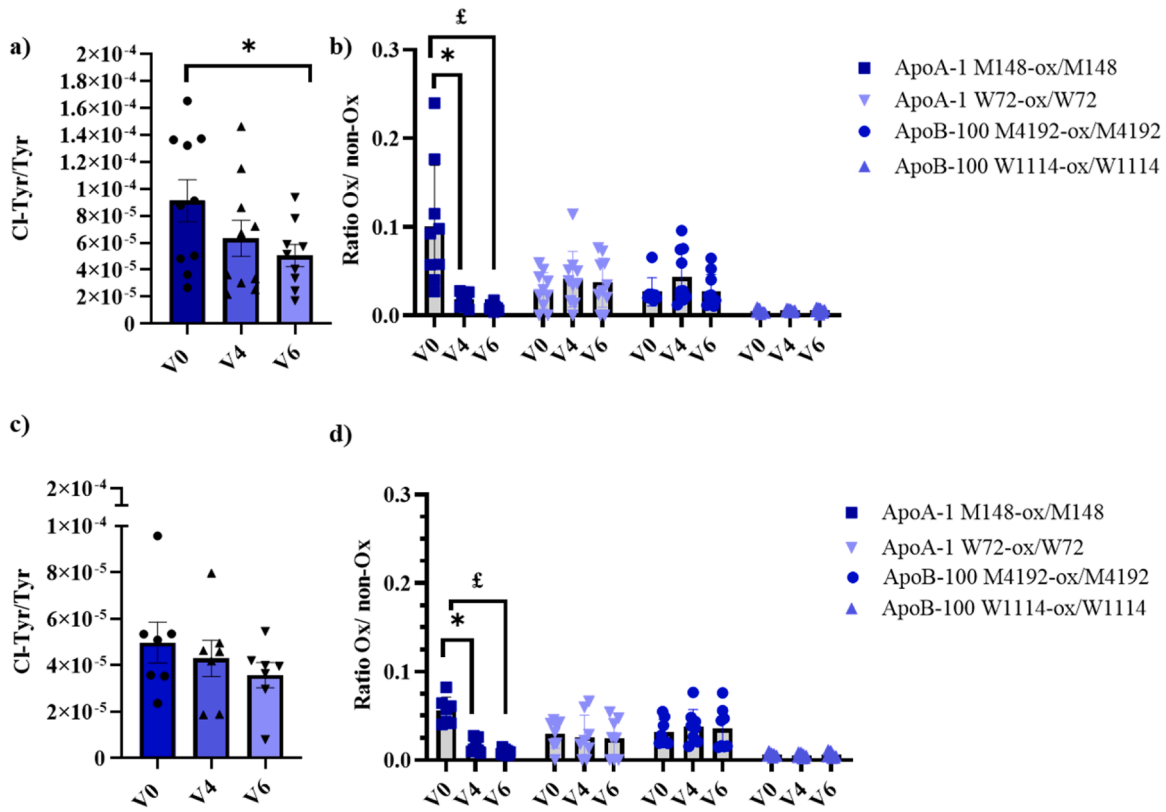

Fig. 12. Comparative changes in Myeloperoxidase (MPO) activity products specifically on levels of oxidized residues in Apolipoprotein A-1 of HDL and Apolipoprotein B-100 of LDL after 6 weeks of daily oral intake of Bacopa monnieri. In group A (400 mg/d) evolution of MPO activity is represented by the 3-chlorotyrosine/tyrosine ratio (Cl-Tyr/Tyr) (Fig. 12a) at V0 (n=10), V4 (n=10) and V6 (n=9). Oxidized ApoA-1 levels (Fig. 12b) are represented by M148-ox/M148 (square, nV0=9, nV4=10, nV6=10) and W72-ox/W72 (downward triangle, nV0=10, nV4=10, nV6=10). Oxidized ApoB-100 levels (Fig. 12b) are represented by M4192-ox/M4192 (circle, nV0=8, nV4=10, nV6=10), and W1114-ox/W1114 (upward triangle, nV0=9, nV4=10, nV6=10); *p<0.05; £p<0.001. Outliers were defined as values >2SD and excluded. Data were represented as mean and SEM. Cl-Tyr/Tyr, M148-ox/M148, M4192-ox/M4192 and W1114-ox/W1114 were subjected to a Kruskal Wallis, followed by a Dunn's test for multiple comparisons while W72-ox/W72 was subjected to a Friedman test. In group B (800 mg/d) evolution of MPO activity is represented by the 3-chlorotyrosine/tyrosine ratio (Cl-Tyr/Tyr) (Fig. 12c) at V0 (n=7), V4 (n=7), and V6 (n=7). Oxidized ApoA-1 levels (Fig. 12d) are represented by M148-ox/M148 (square, nV0=7, nV4=8, nV6=8), and W72-ox/W72 (downward triangle, nV0=8, nV4=8, nV6=8). Oxidized ApoB-100 levels (Fig. 12d) are represented by M4192-ox/M4192 (circle, nV0=8, nV4=8, nV6=8), and W1114-ox/W1114 (upward triangle, nV0=8, nV4=8, nV6=8); *p<0.05; £p<0.001. Outliers were defined as values >2SD and excluded. Data were represented as mean and SEM. Cl-Tyr/Tyr and M148-ox/M148 were subjected to a Kruskal Wallis, followed by a Dunn's test for multiple comparisons while M4192-ox/M4192, W1114-ox/W1114 and W72-ox/W72 were subjected to a Friedman test.

hypochlorous acid. Its activity is positively correlated with endothelial dysfunction, atherosclerotic plaque destabilization, and lipoprotein oxidation [49]. Our observations indicated that oral administration of BM induced a trend towards a progressive decrease in MPO activity products, as evidenced by the 3-chlorotyrosine/tyrosine ratio, which persisted for up to 4 weeks after treatment discontinuation. The MPO-dependent oxidation of HDL (Mox), reflected by the detection of oxidized peptides of ApoA-1 in HDL, results in dysfunctional Mox-HDLs [50], leading to cholesterol-efflux deficiency. Such impairment is typically induced by ApoA-1 oxidation on various Tryptophan and/or Methionine residues [51], which impairs the activation of lecithin-cholesterol acyltransferase (LCAT) [52] and/or the interaction with the macrophage ATP-binding cassette transporter A1 [50,53], leading to cholesterol accumulation in macrophages, the formation of foam cells, and the progression of atherosclerotic plaque [54]. Oral supplementation with BM extracts was associated with a reduction of the oxidized Methionine 148 residue, specifically involved in tertiary structure changes in ApoA-1, impairing its ability to activate LCAT [52,55]. However, this effect appears to be ApoA-1 dependent, as no modifications were observed in ApoB-100 residues of LDL including Methionine residues, which remained unchanged following the ingestion of the BM extract.

Our observations also revealed a significant reduction in the blood pressure profile, characterized by a reduction in systolic and mean arterial pressure in healthy volunteers that persisted over time, with a residual effect up to 4 weeks after treatment discontinuation. Previously, we showed that deletion of the *Aqp1* gene in mice results in low blood pressure [13]. This hypotension phenotype was not explained by dehydration, as already validated in rodents [13] and confirmed in our patients. Again, these results indirectly suggest that oral intake of BM for 6 weeks would be sufficient to block AQP1 in vivo and, to some extent, reproduce the cardiovascular phenotype observed in the *Aqp1* KO mice.

Before AQP1 was identified as a peroxiporin, the impact of BM extracts on blood pressure had already been documented in rodents following intravenous injection of ethanolic BM extracts, as well as in postmenopausal women following oral BM administration [56,57]. Wire myograph studies on rat aortic rings revealed that the BM-induced vasorelaxation was attenuated in endothelium-denuded aortas or under NOS inhibitor (L-NAME) treatment, suggesting that this plant extract acts, at least in part, through NO-dependent endothelial signaling pathways [56]. This finding, combined with our own, suggests that the hypotensive effect of BM could be related to an increase in the bioavailability of NO. This increase may result from the attenuation, by BM extract, of AQP1-dependent ROS entry into endothelial cells. Furthermore, the decreased ROS levels in RBCs, as indicated by the DCFDA test and reflected by reduced MetHb levels, could directly enhance NO levels produced by eNOS in RBCs. This increase in NO production in RBCs was recently shown to contribute to maintain blood

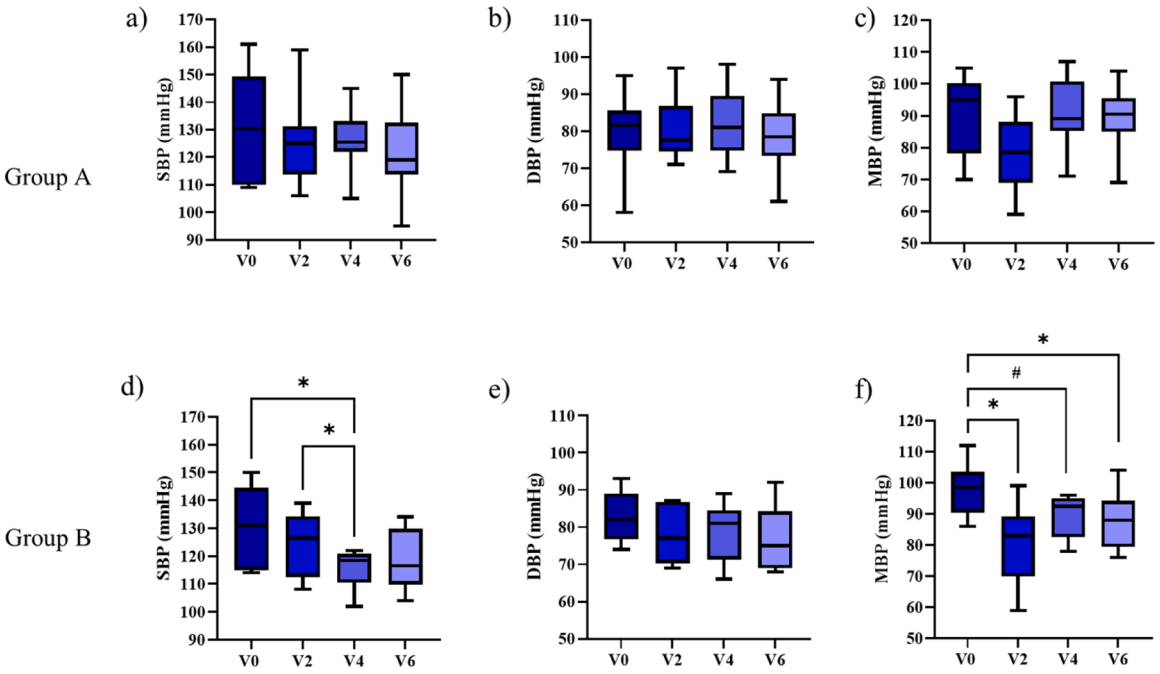

Fig. 13. Changes of Systolic Blood Pressure (SBP), Diastolic Blood Pressure (DBP), and Mean Blood Pressure (MBP) after daily oral intake of BM extracts. Hemodynamic profile in group A with evolution of SBP (nV0=10, nV2=10, nV4=10 and nV6=10; Fig. 13a), DBP (nV0=10, nV2=10, nV4=10 and nV6=10; Fig. 13b) and MBP (nV0=10, nV2=10, nV4=10 and nV6=10; Fig. 13c) and in group B with evolution of SBP (nV0=8, nV2=8, nV4=8 and nV6=8; Fig. 13d), DBP (nV0=8, nV2=8, nV4=8 and nV6=8; Fig. 13e) and MBP (nV0=8, nV2=8, nV4=8 and nV6=8; Fig. 13f) at V0, V2, V4 and V6; *p<0.5; #p<0.01. Data were represented as boxplots and were subjected to a repeated measures one-way ANOVA, followed by a Bonferroni post-hoc test.

Table 4
Assessment of Adverse events.

	Group A (n=10)						Group B (n=8)					
Visits	V1	V2	V3	V4	V5	V6	V1	V2	V3	V4	V5	V6
Abdominal cramps (%)	1 (10)	0 (0)	0 (0)	0 (0)	0 (0)	0 (0)	2 (25)	0 (0)	0 (0)	0 (0)	0 (0)	0 (0)
Excessive thirst (%)	0 (0)	1 (10)	0 (0)	0 (0)	0 (0)	0 (0)	2 (25)	0 (0)	0 (0)	0 (0)	0 (0)	0 (0)
Nausea (%)	1 (10)	0 (0)	0 (0)	0 (0)	0 (0)	0 (0)	1 (12.5)	0 (0)	0 (0)	0 (0)	0 (0)	0 (0)
Polyuria (%)	0 (0)	0 (0)	0 (0)	0 (0)	0 (0)	0 (0)	0 (0)	0 (0)	1 (12.5)	0 (0)	0 (0)	0 (0)
Muscular pain (%)	0 (0)	0 (0)	0 (0)	0 (0)	0 (0)	0 (0)	0 (0)	0 (0)	1 (12.5)	0 (0)	0 (0)	0 (0)
Total/visit (%)	2 (20)	1 (10)	0 (0)	0 (0)	0 (0)	0 (0)	5 (62.5)	0 (0)	2 (25)	0 (0)	0 (0)	0 (0)
Total (%)	3/10 (30)						7/8 (87.5)					

V: Visit; V1: 1 week post-treatment; V2: 2 weeks post-treatment; V3: 3 weeks post-treatment; V4: 6 weeks post-treatment and end of treatment; V5: 2 weeks after the end of treatment; V6: 4 weeks after the end of treatment.

pressure homeostasis [58].

Our study marks the first successful identification of potential metabolites of Bacopaside II associated with oral intake of Bacopa monnieri. The Metabolites 1 and 2 identified in this study appear to have undergone Phase I biotransformation, likely involving deglycosylation, with Metabolite 1 additionally undergoing oxidation [59]. Subsequently, both metabolites seem to have undergone Phase II metabolization, characterized by a sulfation reaction [59]. Currently, there is limited information available regarding the distinct phases of biotransformation of Bacosides in Bacopa monnieri plant extract after oral intake, as well as the potential influence of gut microbiota on these transformations (Phase IV) [60]. In terms of metabolite levels, the group B, which received the highest daily dose, exhibited significantly higher levels of both metabolites in the plasma compared to group A. As mentioned above, docking studies indicate that both metabolites would fit within the AQP1-intra subunit pore, responsible for the transmembrane passage of H_2O_2. Even though Metabolite 1 is quantitatively less abundant than Metabolite 2, Metabolite 1 ($+SO_3$ + OH) appears to have a higher affinity for the AQP1 pore compared to Metabolite 2 ($+SO_3$). As expected, none of these metabolites was present in the parent Bacopa400 extract, and they were no longer detectable 4 weeks after cessation of oral intake, suggesting complete washout.

The persistence of some biological effects (i.e. lower MetHb, decreased M148-ox/M148 ratio in ApoA-1 and blood pressure) despite washout may suggest long-term consequences of decreased oxidant stress (or another yet unidentified effect). Some studies have indeed identified transcriptional effects through NRF2 (Nuclear factor (erythroid-derived2)-like2, or NFE2L2) mediating enduring antioxidant protection after intake of BM extracts [61]. Notably, a key regulator of NRF2 transcriptional activity is the nitrosylation of its inhibitor, Keap-1, aligning with the potentiation of NO signaling by BM inhibition of AQP1 as proposed here. Among antioxidant enzymes upregulated by NRF2 is catalase [62], that converts H_2O_2 into water and oxygen. Increased expression of catalase at the endothelial (or red blood) cell membrane would be expected to degrade extracellular H_2O_2, preventing, e.g. the activation of MPO, consistent with our observations.

Regarding the safety of BM oral intake, no serious adverse effects were reported in this study with the use of this BM extracts, the only problem being gastrointestinal discomfort, which subsided a few weeks after the start of treatment, in line with the existing literature [27,28,

Table 5
Clinical chemistry values over the study period in group A (400mg/d).

Group A (n=10)	V0	V2	V4	V6
Hemogram				
Hemoglobin (g/L)	14.2 (1.2) [a]	13.1 (4.8)	14.3 (1.3)	14.1 (1.5)
Hematocrit (%)	41.7 (3.1) [a]	38.6 (14.1)	41.8 (3.5)	41.4 (4.1)
Platelets	250.6 (46.3) [a]	247.0 (31.6)	246.1 (45.1)	240.2 (38.6)
Renal function				
Creatinine (mg/dL)	0.9 (0.2)[a]	1.0 (0.2)	0.9 (0.2)	0.9 (0.2)
GFR (ml/min)	88.7 (8.7)[a]	87.8 (12.7)	97.0 (11.1)	94.1 (12.0)
Hepatic function				
AST (U/L)	24.3 (12.3)[a]	28.1 (13.4)	22.9 (7.4)	19.5 (4.6)
ALT (U/L)	25.0 (18.4)[a]	26.2 (23.2)	23.0 (13.9)	18.6 (8.2)
GGT (U/L)	19.4 (12.3)[a]	20.5 (13.8)	21.7 (13.9)	18.3 (10.5)
Muscular enzymes				
CK (U/L)	93.8 (53.8)[a]	160.9 (92.5)	106.1 (55.6)	100.4 (36.1)
LDH (UI/L)	186.0 (25.5)[a]	191.7 (24.2)	179.6 (22.7)	173.3 (31.9)
Lipidogram				
Total Cholesterol (mg/dL)	181.3 (41.5)[b]	193.9 (38.7)	197.5 (49.4)	195.3 (44.8)
HDL-Cholesterol (mg/dL)	62.9 (15.3)[b]	61.8 (11.0)	59.2 (10.7)	61.3 (11.6)
LDL-Cholesterol (mg/dL)	104.2 (38.8)[b]	114.4 (39.9)	122.1 (47.4)*	115.6 (40.5)
Triglycerides (mg/dL)	68.4 (15.6)[c]	85.9 (40.3)	81.7 (40.3)	92.5 (37.9)
Ionogram				
Sodium (mM)	125.9 (44.3)[a]	139.8 (2.0)	139.2 (1.9)	139.5 (1.5)
Potassium (mM)	3.7 (1.4)[a]	4.0 (0.3)	4.0 (0.2)	4.0 (0.5)
Bicarbonate (mM)	21.9 (7.8)[a]	33.9 (24.8)	33.2 (25.0)	24.7 (1.4)
Oxidative stress biomarkers				
Plasma peroxides (µM)	549.6 (121.1)[a]	557.4 (109.9)	566.1 (98.5)	565.7 (107.1)
Methemoglobin (a.u)	0.643 (0.065)[a]	–	0.261 (0.040)#	0.183 (0.027)#
MPO activity (Cl Tyrosine/Tyrosine ratio)	9.1×10^{-5} (1.6×10^{-5})[c]		6.3×10^{-5} (1.3×10^{-5})	5.1×10^{-5} (0.83×10^{-5})*
Apolipoprotein A1 M148-ox/M148 ratio	0.10 (0.02) [c]		0.02 (0.00)*	0.01 (0.00)#
Apolipoprotein A1 W72-ox/W72 ratio	0.04 (0.01) [b]		0.05 (0.01)	0.05 (0.01)
Apolipoprotein B-100 M4192-ox/M4192 ratio	0.03 (0.01)[c]		0.04 (0.01)	0.03 (0.01)
Apolipoprotein B-100 W1114-ox/W1114 ratio	0.01 (0.00)[c]		0.01 (0.00)	0.01 (0.00)
Blood pressure				
Systolic blood pressure (mmHg)	131 (20)[b]	125 (15)	127 (11)	122 (16)
Diastolic blood pressure (mmHg)	79 (11)[a]	81 (8)	82 (9)	78 (9)
Mean blood pressure (mmHg)	91 (11)[a]	79 (11)	91 (11)	90 (10)
Potential Bacopaside II metabolites				
Metabolite 1	0.01 (0.01) [c]	–	5.10 (1.56)**	0.00 (0.00)§
Metabolite 2	0.02 (0.01)[c]	–	8.00 (1.70)**	0.01 (0.00)§§

Data are presented as mean (SD) except for Plasma peroxides, Methemoglobin, MPO activity, residues of Apolipoprotein A1 and B100, Metabolites 1 and 2 that are presented as mean (SEM);

[a] Normally distributed data were submitted to a repeated measures one-way ANOVA, followed by a Bonferroni test;

[b] non-normally distributed data were submitted to a Friedman test, followed by a Dunn's multiple comparisons test;

[c] data with outliers (> 2SD) were excluded and were submitted to a Kruskal-Wallis test, followed by a Dunn's test for multiple comparisons.

* $p<0.05$,

** $p<0.01$ and

# $p<0.001$ when compared to V0;

§ $p<0.001$ and

§§ $p<0.0001$ when compared to V4; V: Visit; V0: baseline; V2: 2 weeks post-treatment; V4: 6 weeks post-treatment and end of treatment; V6: 4 weeks after the end of treatment.

63]. Indeed, chronic administration of BM extracts, which have been used for centuries, has never shown any general or even specific biological or cardiovascular side effects in recent, well-conducted trials [27,28,63].

In both groups, we observed a transient increase in LDL-C. Elevated plasma LDL levels are strongly associated with the development of atherosclerosis [64]. However, native LDL is not inherently atherogenic and requires oxidative modifications in order to initiate the disease process [65,66]. Oxidation of ApoB-100-containing lipoproteins represents a critical modification that allows oxidized LDL (ox-LDL) to be recognized by scavenger receptors on macrophages, facilitating the formation of lipid-laden foam cells—an early hallmark of atherosclerotic plaque development [66]. To investigate the specific impact of AQP1 inhibition on ox-LDL, we measured some ApoB-100 residues of LDL that remained unchanged throughout the study, suggesting no significant alterations in LDL oxidation. Nevertheless, such a disruption of the lipid profile was not expected, since the most extensively studied BM extracts, CDRI08 (KeenMind®) or Bacognize®, prepared using a standardized plant extraction technique, showed opposite effects in both rodents and humans [67,68]. Indeed, no disturbance of the lipid profile was observed in healthy volunteers after 6 weeks of treatment [68]. Moreover, a lipid-lowering effect was even observed in patients at high cardiovascular risk, such as postmenopausal women, with a significant reduction in serum triglycerides, cholesterol, and LDL-cholesterol after 4 months of treatment [57].

It is important to consider that the two extracts mentioned in the studies above use specific extraction methods, which may result in a different Bacosides content and purity than other extracts such as Bacopa-400®. Nevertheless, we needed to use Bacopa-400® in this study, as this was the only GMP-certified Bacopa monnieri extract available for sale in Belgium. The unexpected effects observed on the lipid profile may therefore be due to the Bacopa-400® purification technique, resulting in the presence of other compounds responsible for the alteration of the lipid profile.

4.1. Limitation of the study

Technical constraints imposed our study to be conducted as a

Table 6
Clinical chemistry values over the study period in group B (800mg/d).

Group B (n=8)	V0	V2	V4	V6
Hemogram				
Hemoglobin (g/L)	14.8 (1.4) [a]	15.0 (1.3)	14.9 (1.5)	14.5 (1.2)
Hematocrit (%)	42.9 (3.5) [a]	43.8 (3.4)	43.9 (4.4)	41.8 (3.4)
Platelets	257.8 (44.9) [a]	259.4 (33.0)	264.6 (34.1)	255.5 (42.8)
Renal function				
Creatinine (mg/dL)	1.0 (0.1) [a]	1.0 (0.1)	0.9 (0.1)	0.9 (0.1)
GFR (ml/min)	82.8 (18.8) [a]	83.8 (17.8)	87.0 (16.4)	91.2 (17.3)
Hepatic function				
AST (U/L)	28.0 (9.2) [a]	20.0 (3.7)	21.4 (4.3)	24.4 (6.5)
ALT (U/L)	22.8 (8.2) [a]	15.9 (5.2)	14.9 (3.9)*	19.8 (5.2)
GGT (U/L)	17.0 (7.5) [a]	16.4 (6.6)	16.4 (7.2)	15.6 (6.3)
Muscular enzymes				
CK (U/L)	126.9 (55.4) [a]	113.5 (30.6)	127.5 (41.9)	175.1 (58.1)
LDH (UI/L)	182.9 (22.3) [a]	174.8 (22.2)	168.4 (21.3)	171.2 (28.7)
Lipidogram				
Total Cholesterol (mg/dL)	188.2 (29.9) [b]	207.9 (41.2)	210.4 (47.7)	192.4 (31.3)
HDL-Cholesterol (mg/dL)	56.0 (8.8) [b]	57.5 (7.5)	53.4 (7.5)	54.7 (6.0)
LDL-Cholesterol (mg/dL)	111.4 (29.3) [b]	174.8 (22.2) **	168.4 (21.4) *	117.8 (31.6)
Triglycerides (mg/dL)	104.2 (31.6) [c]	112.2 (38.8)	109.8 (42.1)	98.9 (21.2)
Ionogram				
Sodium (mM)	139.6 (1.7) [a]	140.2 (1.8)	135.1 (15.9)	139.9 (2.2)
Potassium (mM)	3.9 (0.3) [a]	4.0 (0.4)	4.0 (0.4)	4.1 (0.3)
Bicarbonate (mM)	23.8 (2.2) [a]	26.0 (2.1)	24.0 (1.4)	24.7 (1.7)
Oxidative stress biomarkers				
Plasma peroxides (μM)	386.2 (80.5)[c]	338.5 (62.7)	352.0 (38.7)	396.4 (30.4)
Methemoglobin (a.u)	0.900 (0.105)[a]	–	0.233 (0.047)#	0.166 (0.042)##
MPO activity (Cl Tyrosine/Tyrosine ratio)	5.0×10^{-5} (0.88×10^{-5}) [c]		4.3×10^{-5} (0.78×10^{-5})	3.6×10^{-5} (0.54×10^{-5})
Apolipoprotein A1 M148-ox/M148 ratio	0.06 (0.01) [b]		0.02 (0.00) *	0.01 (0.00) #
Apolipoprotein A1 W72-ox/W72 ratio	0.03 (0.00) [b]		0.04 (0.01)	0.04 (0.01)
Apolipoprotein B-100 M4192-ox/M4192 ratio	0.03 (0.01) [b]		0.04 (0.01)	0.04 (0.01)
Apolipoprotein B-100 W1114-ox/W1114 ratio	0.01 (0.00)[c]		0.01 (0.00)	0.01 (0.00)
Blood pressure				
Systolic blood pressure (mmHg)	131 (15)[a]	124 (11)§	116 (7)*	119 (11)
Diastolic blood pressure (mmHg)	83 (7)[a]	78 (8)	79 (8)	77 (9)
Mean blood pressure (mmHg)	98 (8)[a]	80 (13)*	89 (7)**	88 (10)*
Potential Bacopaside II metabolites				
Metabolite 1	0.02 (0.01)[c]	–	11.84 (3.50)*	0.01 (0.00)§§
Metabolite 2	0.16 (0.09)[b]	–	29.23 (7.90)##	0.03 (0.00)§§

Data are presented as mean (SD) except for Plasma peroxides, Methemoglobin, MPO activity, residues of Apolipoprotein A1 and B100, Metabolites 1 and 2 that are presented as mean (SEM);

[a] Normally distributed data were submitted to a repeated measure one-way ANOVA, followed by a Bonferroni test;

[b] non-normally distributed data were submitted to a Friedman test, followed by a Dunn's multiple comparisons test;

[c] data with outliers (> 2SD) were excluded and were submitted to a Kruskal-Wallis test, followed by a Dunn's test for multiple comparisons .

* $p<0.05$,

** $p<0.01$,

# $p<0.001$ and

$p<0.0001$ when compared to V0;

§ $p<0.01$ and

§§ $p<0.0001$ compared to V4; V: Visit; V0: baseline; V2: 2 weeks post-treatment; V4: 6 weeks post-treatment and end of treatment; V6: 4 weeks after the end of treatment.

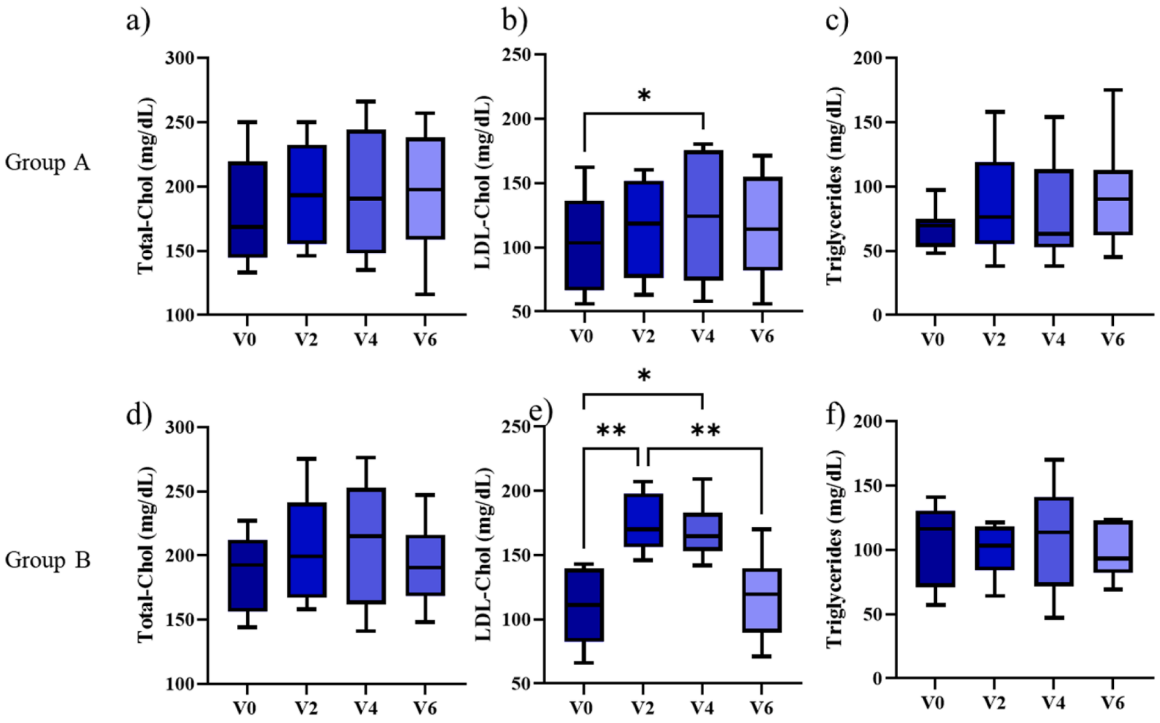

Fig. 14. Changes of total cholesterol, LDL-cholesterol, and triglycerides after daily oral intake of BM extracts. The lipid profile evolution in Group A included total cholesterol (nV0=10, nV2=10, nV4=10 and nV6=10; Fig. 14a), LDL-cholesterol (nV0=10, nV2=10, nV4=10 and nV6=10; Fig. 14b) and triglycerides (nV0=8, nV2=10, nV4=10 and nV6=10; Fig. 14c); *p<0.5. Data were presented as boxplots. Statistical analysis for total cholesterol and LDL-cholesterol were performed using a Friedman test followed by a Dunn's test for multiple comparisons. Statistical analysis for triglycerides was performed using the Kruskal-Wallis test. Two outliers (>2SD) were excluded at V0 for triglycerides.

monocentric trial, which may raise questions. Specifically, we required freshly drawn blood for ROS detection using the DCFDA test. Although the appropriate sample size was calculated *a priori*, we included a relatively small number of healthy volunteers, with two exclusions in group B due to COVID-19. Replicating these findings in larger populations would be valuable. Also, healthy volunteers naturally display low oxidative stress, which may have limited the observable decrease with our intervention. Our study spanned 6 weeks, whereas other clinical trials involved daily intake for 12 weeks [69,70]. These different durations may contribute to the modest effect of oral BM on some parameters, such as plasma peroxides in our study. Moreover, BM extracts being derived from the entire plant, they may contain a diverse array of compounds so that their effects may not exclusively be credited to Bacopaside II alone. Developing a galenic formulation of pure Bacopaside II could offer a more standardized therapeutic approach.

5. Conclusion

In conclusion, our findings suggest that the pharmacological blockade of AQP1 by Bacopaside II or its derivatives, which is associated with a preserved overall redox status of healthy volunteers may hold promise for future therapeutic interventions in cardiovascular diseases.

Data sharing

The data supporting the findings of this study will be made accessible upon request. Interested researchers should contact the corresponding author to arrange access. An appropriate data sharing agreement, ensuring compliance with ethical guidelines and data protection regulations, must be established prior to the release of any data.

Competency in medical knowledge:

Endothelial dysfunction, marked by excessive production of ROS and reduced NO bioavailability, is a key precursor to atherosclerotic lesions and vascular diseases. Despite various efforts, the use of exogenous antioxidants has not been effective in reducing atherosclerosis. We recently identified AQP1 as a peroxiporin. Targeting AQP1 to limit the transmembrane passage of hydrogen peroxide—thereby reducing oxidative stress and enhancing NO bioavailability—via a specific inhibitor, may present a novel therapeutic strategy for treating endothelial dysfunction.

Translational outlook:

This study highlights the potential of BM containing Bacopaside II, as a novel therapeutic approach for reducing systemic oxidative stress, improving HDL function, and lowering blood pressure. The identification of Bacopaside II metabolites and their likely binding to the AQP1 pore suggests that the beneficial effects observed are due to the modulation of AQP1 activity, rather than direct ROS scavenging. Given these promising results, targeting AQP1 could provide a valuable strategy for early intervention in endothelial dysfunction. However, exploring this potential with larger cohorts and longer treatment durations seems essential to confirm these findings.

Funding sources

King Baudouin Foundation and FNRS.

CRediT authorship contribution statement

Hasnae Boughaleb: Writing – original draft, Visualization, Software, Project administration, Methodology, Investigation, Formal analysis. **Roxane Verdoy:** Writing – review & editing, Formal analysis. **Amandine Pochet:** Visualization, Validation, Software, Formal analysis. **Nathalie Fabian:** Writing – review & editing, Validation, Software, Methodology, Formal analysis. **Ramona Bella:** Writing – review & editing, Validation, Software, Methodology, Formal analysis. **Gopinath Muruganandam:** Writing – review & editing, Visualization, Validation,

Software, Methodology, Formal analysis. **Raphaël Frédérick:** Writing – review & editing, Visualization, Validation. **Karim Zouaoui Boudjeltia:** Writing – review & editing, Validation, Methodology, Formal analysis. **Axelle Bourez:** Writing – review & editing, Validation, Software, Methodology, Formal analysis. **Cédric Delporte:** Writing – review & editing, Validation, Methodology. **Pierre Van Antwerpen:** Writing – review & editing, Validation, Methodology. **Annie Robert:** Writing – review & editing, Validation, Methodology. **Vincent Haufroid:** Writing – review & editing, Validation, Methodology. **Joseph P. Dewulf:** Writing – review & editing, Visualization, Validation, Software, Methodology, Formal analysis. **Jean-Luc Balligand:** Writing – review & editing, Visualization, Validation, Supervision, Resources, Methodology, Investigation, Funding acquisition, Conceptualization. **Virginie Montiel:** Writing – review & editing, Visualization, Validation, Supervision, Resources, Project administration, Methodology, Investigation, Funding acquisition, Conceptualization.

Declaration of competing interest

None of the authors have conflicts of interests to declare

Acknowledgements

We thank Noureddine Khaddamallah and Victor Stamar, master's students in biomedical sciences, for their contributions to the BacOxy study, including patient recruitment, follow-up, and data entry. We thank the intensive care unit nurses and assistants for their support in the study's conduct.

Supplementary materials

Supplementary material associated with this article can be found, in the online version, at doi:10.1016/j.arres.2025.100126.

Data availability

Data will be made available on request.

References

[1] S. Srikanth, P. Deedwania, Management of dyslipidemia in patients with hypertension, diabetes, and metabolic syndrome, Current Hypertension Reports 18 (10) (2016) 76.
[2] S. Jebari-Benslaiman, U. Galicia-García, A. Larrea-Sebal, J.R. Olaetxea, I. Alloza, K. Vandenbroeck, et al., Pathophysiology of atherosclerosis, Int J Mol Sci. 23 (6) (2022) 3346.
[3] Eurostat. eurostat. 2024 [cited 2024 Jul 9]. Cardiovascular diseases statistics. Available from: https://ec.europa.eu/eurostat/statistics-explained/index.php?title=Cardiovascular_diseases_statistics.
[4] Q. Chen, Q. Wang, J. Zhu, Q. Xiao, L. Zhang, Reactive oxygen species: key regulators in vascular health and diseases: ROS in vascular diseases, British Journal of Pharmacology 175 (8) (2018) 1279–1292.
[5] U. Förstermann, T. Münzel, Endothelial nitric oxide synthase in vascular disease: from marvel to menace, Circulation 113 (13) (2006) 1708–1714.
[6] E.J. Tsai, Y. Liu, N. Koitabashi, D. Bedja, T. Danner, J.F. Jasmin, et al., Pressure-overload-induced subcellular relocalization/oxidation of soluble guanylyl cyclase in the heart modulates enzyme stimulation, Circulation research 110 (2) (2012) 295–303.
[7] C. Farah, L.Y.M. Michel, JL. Balligand, Nitric oxide signalling in cardiovascular health and disease, Nature Reviews. Cardiology 15 (5) (2018) 292–316.
[8] G. Pizzino, N. Irrera, M. Cucinotta, G. Pallio, F. Mannino, V. Arcoraci, et al., Oxidative stress: harms and benefits for Human health, Oxidative Medicine and Cellular longevity 2017 (2017) 8416763.
[9] H. Sies, Hydrogen peroxide as a central redox signaling molecule in physiological oxidative stress: oxidative eustress, Redox Biology 11 (2017) 613–619.
[10] G.M. Preston, T.P. Carroll, W.B. Guggino, P. Agre, Appearance of water channels in Xenopus oocytes expressing red cell CHIP28 protein, Science (New York, N.Y.) 256 (5055) (1992) 385–387.
[11] AS. Verkman, Aquaporins in Clinical medicine, Annual Review of medicine 63 (2012) 303–316.
[12] T.L. Butler, C.G. Au, B. Yang, J.R. Egan, Y.M. Tan, E.C. Hardeman, et al., Cardiac aquaporin expression in humans, rats, and mice, American Journal of Physiology. Heart and Circulatory Physiology 291 (2) (2006) H705–H713.
[13] V. Montiel, E. Leon Gomez, C. Bouzin, H. Esfahani, M. Romero Perez, I. Lobysheva, et al., Genetic deletion of aquaporin-1 results in microcardia and low blood pressure in mouse with intact nitric oxide-dependent relaxation, but enhanced prostanoids-dependent relaxation, Pflugers Archiv : European Journal of Physiology 466 (2) (2014) 237–251.
[14] A.J. Yool, EM. Campbell, Structure, function and translational relevance of aquaporin dual water and ion channels, Molecular Aspects of Medicine 33 (5) (2012) 553–561.
[15] G.P. Bienert, F. Chaumont, Aquaporin-facilitated transmembrane diffusion of hydrogen peroxide, Biochimica et biophysica acta 1840 (5) (2014) 1596–1604.
[16] V. Montiel, R. Bella, L.Y.M. Michel, H. Esfahani, D. De Mulder, E.L. Robinson, et al., Inhibition of aquaporin-1 prevents myocardial remodeling by blocking the transmembrane transport of hydrogen peroxide, Science Translational Medicine 12 (564) (2020) eaay2176.
[17] J.V. Pei, M. Kourghi, M.L. De Ieso, E.M. Campbell, H.S. Dorward, J.E. Hardingham, et al., Differential inhibition of water and ion channel activities of mammalian aquaporin-1 by two structurally related bacopaside compounds derived from the medicinal plant Bacopa monnieri, Molecular Pharmacology 90 (4) (2016) 496–507.
[18] E. Smith, H.M. Palethorpe, Y. Tomita, J.V. Pei, A.R. Townsend, T.J. Price, et al., The purified extract from the medicinal plant bacopa monnieri, bacopaside II, inhibits growth of colon cancer cells In vitro by, Inducing Cell Cycle Arrest and Apoptosis. Cells. 7 (7) (2018) 81.
[19] C. Sivaramakrishna, C.V. Rao, G. Trimurtulu, M. Vanisree, GV. Subbaraju, Triterpenoid glycosides from *Bacopa monnieri*, Phytochemistry 66 (23) (2005) 2719–2728.
[20] V.C. Sekhar, G. Viswanathan, S. Baby, Insights into the molecular aspects of neuroprotective bacoside A and bacopaside I, CN 17 (5) (2019) 438–446.
[21] R.L. Crisp, R.E. Maltaneri, D.C. Vittori, L. Solari, D. Gammella, G. Schvartzman, et al., Red blood cell aquaporin-1 expression is decreased in hereditary spherocytosis, Annals of Hematology 95 (10) (2016) 1595–1601.
[22] E. von Elm, D.G. Altman, M. Egger, S.J. Pocock, P.C. Gøtzsche, J. P. Vandenbroucke, et al., The strengthening the reporting of Observational Studies in Epidemiology (STROBE) Statement: guidelines for reporting observational studies, International Journal of Surgery (London, England) 12 (12) (2014) 1495–1499.
[23] V. Montiel, I. Lobysheva, L. Gérard, M. Vermeersch, D. Perez-Morga, T. Castelein, et al., Oxidative stress-induced endothelial dysfunction and decreased vascular nitric oxide in COVID-19 patients, EBioMedicine 77 (2022) 103893.
[24] B. Ward, J.C. Yombi, J.L. Balligand, P.D. Cani, J.F. Collet, J. de Greef, et al., HYGIEIA: HYpothesizing the genesis of infectious diseases and epidemics through an integrated systems biology approach, Viruses 14 (7) (2022) 1373.
[25] TA. Halgren, Merck molecular force field. II. MMFF94 van der Waals and electrostatic parameters for intermolecular interactions, Journal of Computational Chemistry 17 (5–6) (1996) 520–552.
[26] C. Delporte, T. Franck, C. Noyon, D. Dufour, A. Rousseau, P. Madhoun, et al., Simultaneous measurement of protein-bound 3-chlorotyrosine and homocitrulline by LC–MS/MS after hydrolysis assisted by microwave: application to the study of myeloperoxidase activity during hemodialysis, Talanta 99 (2012) 603–609.
[27] K. Pravina, K.R. Ravindra, K.S. Goudar, D.R. Vinod, A.J. Joshua, P. Wasim, et al., Safety evaluation of BacoMind in healthy volunteers: a phase I study, Phytomedicine : International Journal of Phytotherapy and Phytopharmacology 14 (5) (2007) 301–308.
[28] Dave UP, Dingankar SR, Saxena VS, Joseph JA, Bethapudi B, Agarwal A, et al. An open-label study to elucidate the effects of standardized Bacopa monnieri extract in the management of symptoms of attention-deficit hyperactivity disorder in children.
[29] P.A. Harris, R. Taylor, B.L. Minor, V. Elliott, M. Fernandez, L. O'Neal, et al., The REDCap consortium: building an international community of software platform partners, Journal of Biomedical Informatics 95 (2019) 103208.
[30] P.A. Harris, R. Taylor, R. Thielke, J. Payne, N. Gonzalez, JG. Conde, Research electronic data capture (REDCap)—A metadata-driven methodology and workflow process for providing translational research informatics support, Journal of Biomedical Informatics 42 (2) (2009) 377–381.
[31] A.W.C. Man, H. Li, N. Xia, Impact of lifestyles (Diet and Exercise) on vascular health: oxidative stress and endothelial function, Oxidative Medicine and Cellular Longevity 2020 (2020) 1496462.
[32] T. Nakamura, M. Uematsu, T. Yoshizaki, T. Kobayashi, Y. Watanabe, K. Kugiyama, Improvement of endothelial dysfunction is mediated through reduction of remnant lipoprotein after statin therapy in patients with coronary artery disease, Journal of Cardiology 75 (3) (2020) 270–274.
[33] J.V. Mombouli, PM. Vanhoutte, Endothelial dysfunction: from physiology to therapy, Journal of molecular and cellular cardiology 31 (1) (1999) 61–74.
[34] I.V.G. Silva, R.C. de Figueiredo, DRA. Rios, Effect of different classes of antihypertensive drugs on endothelial function and inflammation, International Journal of Molecular Sciences 20 (14) (2019) 3458.
[35] JB. Su, Vascular endothelial dysfunction and pharmacological treatment, World Journal of Cardiology 7 (11) (2015) 719–741.
[36] N. Katsiki, C. Manes, Is there a role for supplemented antioxidants in the prevention of atherosclerosis? Clinical Nutrition (Edinburgh, Scotland) 28 (1) (2009) 3–9.
[37] S.K. Myung, W. Ju, B. Cho, S.W. Oh, S.M. Park, B.K. Koo, et al., Efficacy of vitamin and antioxidant supplements in prevention of cardiovascular disease: systematic review and meta-analysis of randomised controlled trials, BMJ (Clinical Research ed.) 346 (2013) f10.

[38] D.J.A. Jenkins, J.D. Spence, E.L. Giovannucci, Y.I. Kim, R.G. Josse, R. Vieth, et al., Supplemental vitamins and minerals for cardiovascular disease prevention and treatment: JACC Focus Seminar, Journal of the American College of Cardiology 77 (4) (2021) 423–436.

[39] Y. Ye, J. Li, Z. Yuan, Effect of antioxidant vitamin supplementation on cardiovascular outcomes: a meta-analysis of randomized controlled trials, PloS one 8 (2) (2013) e56803.

[40] J. Yang, Y. Zhang, X. Na, A. Zhao, β-carotene supplementation and risk of cardiovascular disease: A systematic review and meta-analysis of randomized controlled trials, Nutrients 14 (6) (2022) 1284.

[41] S. Keramat, H. Sharebiani, M. Patel, B. Fazeli, A. Stanek, The potential role of antioxidants in the treatment of peripheral arterial disease: A systematic review, Antioxidants (Basel, Switzerland) 11 (11) (2022) 2126.

[42] NS. Bryan, Nitric oxide enhancement strategies, Future Science OA 1 (1) (2015) FSO48.

[43] F. Dei Zotti, R. Verdoy, D. Brusa, Lobysheva II, J.L. Balligand, Redox regulation of nitrosyl-hemoglobin in human erythrocytes, Redox Biology 34 (2020) 101399.

[44] L. Massaccesi, E. Galliera, M.M. Corsi Romanelli, Erythrocytes as markers of oxidative stress related pathologies, Mechanisms of Ageing And Development 191 (2020) 111333.

[45] C. Huang, J. Gao, T. Wei, W. Shen, Angiotensin II-induced erythrocyte senescence contributes to oxidative stress, Rejuvenation Research 25 (1) (2022) 30–38.

[46] J. Mohanty, E. Nagababu, JM. Rifkind, Red blood cell oxidative stress impairs oxygen delivery and induces red blood cell aging, Front Physiol 5 (84) (2014) [cited 2024 Jul 9]Available from: https://www.frontiersin.org/journals/physiology/articles/10.3389/fphys.2014.00084/full.

[47] V.V. Bamm, M.E.L. Henein, S.L.J. Sproul, D.K. Lanthier, G. Harauz, Potential role of ferric hemoglobin in MS pathogenesis: effects of oxidative stress and extracellular methemoglobin or its degradation products on myelin components, Free Radical Biology and Medicine 112 (2017 1) 494–503.

[48] J. Umbreit, Methemoglobin–it's not just blue: a concise review, American Journal of Hematology 82 (2) (2007) 134–144.

[49] C. Tangeten, K. Zouaoui Boudjeltia, C. Delporte, P. Van Antwerpen, K. Korpak, Unexpected role of MPO-oxidized LDLs in atherosclerosis: In between, Inflammation and Its Resolution. Antioxidants. 11 (5) (2022) 874.

[50] C. Bergt, S. Pennathur, X. Fu, J. Byun, K. O'Brien, T.O. McDonald, et al., The myeloperoxidase product hypochlorous acid oxidizes HDL in the human artery wall and impairs ABCA1-dependent cholesterol transport, Proceedings of the National Academy of Sciences of the United States of America 101 (35) (2004) 13032–13037.

[51] C. Coremans, C. Delporte, F. Cotton, P.V.D. Borne, K.Z. Boudjeltia, PV. Antwerpen, Mass spectrometry for the monitoring of lipoprotein oxidations by myeloperoxidase in cardiovascular diseases, Molecules 26 (17) (2021) [cited 2024 Aug 25]Available from: https://www.ncbi.nlm.nih.gov/pmc/articles/PMC8434463/.

[52] B. Shao, G. Cavigiolio, N. Brot, M.N. Oda, JW. Heinecke, Methionine oxidation impairs reverse cholesterol transport by apolipoprotein A-I, Proceedings of the National Academy of Sciences 105 (34) (2008) 12224–12229.

[53] B. Shao, C. Tang, A. Sinha, P.S. Mayer, G.D. Davenport, N. Brot, et al., Humans with atherosclerosis have impaired ABCA1 cholesterol efflux and enhanced high-density lipoprotein oxidation by myeloperoxidase, Circulation Research 114 (11) (2014) 1733–1742.

[54] E. Favari, A. Chroni, U.J.F. Tietge, I. Zanotti, J.C. Escolà-Gil, F. Bernini, Cholesterol efflux and reverse Cholesterol transport, in: A. von Eckardstein, D. Kardassis (Eds.), High Density Lipoproteins: From Biological Understanding to Clinical Exploitation, Springer International Publishing, Cham, 2015, pp. 181–206, https://doi.org/10.1007/978-3-319-09665-0_4 [cited 2024 Aug 28].Available from:.

[55] G.J. Zhao, K. Yin, Fu Y chang, C.K. Tang, The interaction of ApoA-I and ABCA1 triggers signal transduction pathways to mediate efflux of cellular lipids, Molecular medicine (Cambridge, Mass) 18 (2) (2012) 149–158.

[56] N. Kamkaew, C.N. Scholfield, K. Ingkaninan, P. Maneesai, H.C. Parkington, M. Tare, et al., Bacopa monnieri and its constituents is hypotensive in anaesthetized rats and vasodilator in various artery types, Journal of Ethnopharmacology 137 (1) (2011) 790–795.

[57] Kala M, Kumar T, Singh H. Effect of bacosides enriched standardized extract of Bacopa monniera (BESEB-CDRI-08) on lipid profile and blood pressure of postmenopausal women: a pilot study.

[58] F. Leo, T. Suvorava, S.K. Heuser, J. Li, A. LoBue, F. Barbarino, et al., Red blood cell and endothelial eNOS independently regulate circulating nitric oxide metabolites and blood pressure, Circulation 144 (11) (2021 Sep) 870–889.

[59] S. Phang-Lyn, VA. Llerena, Biochemistry, biotransformation. StatPearls, StatPearls Publishing, 2023 [cited 2024 May 8]. Available from: https://www.ncbi.nlm.nih.gov/books/NBK544353/.

[60] G. Minale, T. Saesong, P. Temkitthawon, N. Waranuch, N. Nuengchamnong, K. Chootip, et al., Characterization of metabolites in plasma, urine and feces of healthy participants after taking Brahmi essence for twelve weeks using LC-ESI-QTOF-MS metabolomic approach, Molecules (Basel, Switzerland) 26 (10) (2021) 2944.

[61] S. Ghosh, V. Kumar, H. Mukherjee, S. Saini, S. Gupta, S. Chauhan, et al., Assessment of the mechanistic role of an Indian traditionally used ayurvedic herb *Bacopa monnieri (L.)*Wettst. For ameliorating oxidative stress in neuronal cells, Journal of Ethnopharmacology 328 (2024 28) 117899.

[62] I. Y, Y. N, M. S, Y. T, T.T. Y, A. A, et al., Compensatory role of the Nrf2-ARE pathway against paraquat toxicity: relevance of 26S proteasome activity, Journal of pharmacological Sciences 129 (3) (2015) [cited 2024 Sep 30]Available from: https://pubmed.ncbi.nlm.nih.gov/26598004/.

[63] T. Ma, S. Jayaraman, K.S. Wang, Y. Song, B. Yang, J. Li, et al., Defective dietary fat processing in transgenic mice lacking aquaporin-1 water channels, American Journal of Physiology. Cell Physiology 280 (1) (2001) C126–C134.

[64] Low-density lipoproteins cause atherosclerotic cardiovascular disease. 1. Evidence from genetic, epidemiologic, and clinical studies. A consensus statement from the European Atherosclerosis Society Consensus Panel | European Heart Journal | Oxford Academic. [cited 2024 Sep 7]. Available from: https://academic.oup.com/eurheartj/article/38/32/2459/3745109.

[65] M. Munno, A. Mallia, A. Greco, G. Modafferi, C. Banfi, S. Eligini, Radical oxygen species, oxidized low-density lipoproteins, and lectin-like oxidized low-density lipoprotein receptor 1: A vicious circle in atherosclerotic process, Antioxidants 13 (5) (2024) 583.

[66] C. Khatana, N.K. Saini, S. Chakrabarti, V. Saini, A. Sharma, R.V. Saini, et al., Mechanistic insights into the oxidized low-density lipoprotein-induced atherosclerosis, Oxidative Medicine and Cellular Longevity 2020 (2020 Sep) 5245308.

[67] V. Kamesh, T. Sumathi, Antihypercholesterolemic effect of Bacopa monniera linn. On high cholesterol diet induced hypercholesterolemia in rats, Asian Pacific Journal of Tropical Medicine 5 (12) (2012) 949–955.

[68] N. Kumar, L.G. Abichandani, V. Thawani, K.J. Gharpure, M.U.R. Naidu, G. Venkat Ramana, Efficacy of standardized extract of bacopa monnieri (Bacognize®) on cognitive functions of medical students: A six-week, randomized placebo-controlled trial, Evidence-Based Complementary and Alternative Medicine : eCAM 2016 (2016) 4103423.

[69] A. Morgan, J. Stevens, Does Bacopa monnieri improve memory performance in older persons? Results of a randomized, placebo-controlled, double-blind trial, Journal of Alternative and Complementary Medicine (New York, N.Y.) 16 (7) (2010) 753–759.

[70] C. Harshad, Rajeshwari P. Barbhaiya, Vinod S. Desai, K. Saxena, A. Pravina, Amit, Efficacy and tolerability of BacoMind® on memory improvement in elderly participants - A double blind placebo controlled study, Journal of Pharmacology and Toxicology (2008) 425–434.